The Vein Hosted Copper Deposits of the Allihies Mining Area, Southwest Ireland – A New Structural and Chronological Evaluation

Jürgen Lang[1]*, Patrick A. Meere[1], Richard P. Unitt[1], Sean C. Johnson[2], Giulio Solferino[3], Koen Torremans[2], David Selby[4,5] & Roisin Kyne[6]

[1] *Irish Centre for Research in Applied Geosciences (iCRAG), School of Biological, Earth and Environmental Sciences, University College Cork, Distillery Fields, North Mall, Cork, Ireland*

[2] *Irish Centre for Research in Applied Geosciences (iCRAG), University College Dublin, Belfield, Dublin 4, Ireland*

[3] *Department of Earth Sciences, Royal Holloway University of London, Egham, Surrey, United Kingdom*

[4] *Department of Earth Sciences, University of Durham, Durham, United Kingdom*

[5] *State Key Laboratory of Geological Processes and Mineral Resources, School of Earth Resources, China University of Geoscience Wuhan, Hubei Province, 430074, China*

[6] *Teck Resources Limited, Suite 3300, Bentall 5. 550 Burrard Street, Vancouver, B.C., Canada, V6C 0B3*

**Corresponding author (e-mail: juergen.lang@icrag-centre.org)*

ORCiDs of authors preceded by their initials (optional):

J.L. https://orcid.org/0000-0003-0086-0193

P.M. https://orcid.org/0000-0001-7686-2641

R.U. https://orcid.org/0000-0002-7504-1451

K.T. http://orcid.org/0000-0002-5127-5050

Abbreviated title: The Copper Deposits of Allihies, SW Ireland

Keywords: quartz veins, Variscan Orogeny, copper mineralisation, drone mapping, Munster Basin & South Munster Basin, fluid inclusions, Re-Os geochronology

Abstract: This paper presents new data for historic vein-hosted copper sulphide deposits in the Upper Palaeozoic Munster and South Munster Basins of southwest Ireland. Detailed mapping, 3D modelling, fluid inclusion microthermometry and geochronology from the Allihies area of the Beara Peninsula, have led to a new interpretation of the timing and development of ore mineralisation. Macro- and microstructural studies reveal that the ore-bearing, mainly E-W striking quartz veins are directly related to early extensional, basinal normal faults. Molybdenite Re-Os dating of the main-stage Cu lode yield ages from 367.3 ± 5.5 to 366.4 ± 1.9 Ma. This early vein system experienced subsequent late Carboniferous Variscan deformation, including cleavage development, sinistral SW-NE strike slip faulting, cataclastic deformation and recrystallization. The new timing of Cu mineralisation in SW Ireland has major implications for its relationship to the base metal deposits of the Irish Midlands. *(end of abstract)*

The mineral deposits of the Irish Variscan fold/thrust belt have been exploited for over 3500 years (Williams 1991). In southwest Ireland copper has been mined as far back as the Bronze Age (O'Brien 1987). In 1812, malachite stained cliff faces at Dooneen on the Beara Peninsula (Fig. 1 and 2) led to the discovery of significant copper lodes (Blenkinsop 1902; Reilly 1986). As miners progressed further inland, they uncovered metal-rich, steeply dipping, E-W striking quartz veins in the vicinity of Allihies (Fig. 1 and 2). The biggest vein was worked at Mountain Mine which at the time became the largest copper mine in the region with a total estimated 284,500 tonnes ore extracted (O'Brien 1959).

This paper focusses on the copper deposits of the Allihies mining district in West Cork (Fig. 2) where previous authors studied the structure and chronology of the vein mineralisation (Sheridan 1964; Sanderson 1984; Spinks *et al.* 2016).

Geological Setting

Between the Middle and early Upper Devonian, north-south crustal extension led to the development of a half-graben structure in southern Ireland that comprises the Munster Basin (Naylor & Jones 1967). The northern bounding structure of this intracratonic basin has been described as the east-west trending, listric Coomnacronia-Killarney-Mallow Fault Zone (Fig. 1; Naylor & Jones 1967; Capewell 1975; Price & Todd 1988; Meere 1995; Vermeulen *et al.* 2000; Landes *et al.* 2003; MacCarthy 2007; Ennis *et al.* 2015) or the Dingle Bay-Galtee Fault Zone Williams (2000).

The lithostratigraphic nomenclature of the basin sediments is described in detail by MacCarthy 1990, MacCarthy *et al.* 2002 and Pracht & Sleeman 2002. Late Middle to Upper Devonian alluvial and fluvial siliciclastic sediments derived mainly from the north were transported into the Munster Basin (MacCarthy 1990). These 'Upper Old Red Sandstone' sediments formed a basinal infill of over 6 km (Meere & Banks 1997). MacCarthy (1990) divided these siliciclastic sediments into 5 facies associations which evolved from early basin margin alluvial fans to floodplain-sheetfloods and ephemeral lakes.

Towards the end of the Devonian the formation of another east-west trending fault system, the Cork-Kenmare Fault Zone (Fig. 1) resulted in continuous subsidence of the South Munster Basin (MacCarthy 2007). This was accompanied by a marine transgression from the south with resulting accumulation of marine siliciclastics within the South Munster Basin and limestones on a more stable platform to the north (Fig. 1; MacCarthy 2007).

At the end of the Carboniferous NNW-directed compression terminated sedimentation in the region and marked the beginning of the Variscan Orogeny (Sanderson 1984; Ford 1987; Meere 1995; Quinn *et al.* 2005). Bulk shortening of over 52 % was achieved by pervasive cleavage development followed by kilometre scale buckling and faulting (Cooper & Trayner 1986; Ford 1987). This resulted in the reactivation of high-angle basin-controlling faults (Price & Todd 1988). In the west of the Munster Basin, Meere (1995) identified NE-SW-trending reverse faults, as well as rarer NW-SE-trending strike slip faults. The sediments underwent metamorphism to sub-greenschist facies (Meere 1995).

E-W and ENE-WNW trending faults were interpreted by Wen *et al.* (1996) as late orogenic events. Daltry (1985) described a possible relationship of these fault systems with Post-Hercynian (Post-Variscan) wrench movements, associated with the North Atlantic opening in the Permian.

A series of minor sheet-like intrusions of mainly alkali basalts, trachytes and phonolites have been found along the northern coastline of Beara Peninsula (Pracht 2000; Fig. 1). These basalts are interpreted as surficial intrusions during the subsidence phase of the Munster

Basin. Pipe-like lamprophyric intrusions dated at 314.44 ± 1.00 Ma (Ar/Ar phlogopite, Quinn *et al.* 2005) occur at Black Ball Head (5.6 km south of Allihies), which were formed during the early Variscan compression (Pracht & Kinnaird 1995; Pracht 2000).

The Allihies Mining District is located near the western end of the Beara Peninsula (Fig. 2). The predominant lithologies are purple and green siltstones and sandstones of the Caha Mountain Formation (MacCarthy *et al.* 2002). The Caha Mountain Formation can be subdivided into the Allihies Sandstone Member, which mainly outcrops north of Mountain Mine (Fig. 2) and has an approximate thickness of 1200 m, and the underlying Ballydonegan Slate Member (south of Mountain Mine) that has an approximate thickness of 1500 m (Reilly 1986).

The Allihies copper mines are positioned on the northern limb of the Beara Anticline (Sheridan 1964). Around the mines, third-order open symmetrical folds with wavelengths of 90 to 150 m, trending SW-NE can be found associated with fault zones following similar strike (Reilly 1986; Fig. 2). Penetrative cleavage is sub-vertical and strikes SW-NE (Reilly 1986). The Cornish Village Fault is one of the rare NW-trending faults and was previously interpreted as a pre-mineralisation structure (Reilly 1986; Fig. 2).

There has been differing opinions about the timing of the vein structures and the copper mineralisation of the Allihies region. For example, mineralised veins were considered to post-date the barren veins and Variscan compression tectonics (Sheridan 1964). In direct contrast is the observation by Sanderson (1984) that mineralised (chalcopyrite and siderite) N-S trending quartz veins are both strongly folded and cleaved, suggesting a pre/syn-Variscan age. Sanderson (1984) also proposed that the east-west veins, which include the main lodes of the mining area, were formed in association with the cleavage development and the folding. Rogers (2002) divided the quartz veins of the Beara Peninsula into 3 different genetic events; early buckled veins, syn-buckled (syn-Variscan) and late stage extension. Wen *et al.* (1996) and Spinks *et al.* (2016) suggested remobilisation of sediment-hosted sulphides into late- or post-Variscan quartz veins.

At Mountain Mine Reilly (1986; Fig. 2) describes the major copper lodes, the E-W Lode, N-S Lode and New E-W Lode together defining a Z-shaped surficial outcrop. On the surface, these lodes are up to 18 m wide and 240 m long with bleached, altered, wall-rock zones up to 21 m in width. The mineralisation has been described in detail by Sheridan (1964) as consisting of mainly chalcopyrite, tetrahedrite and bornite within “compact silica” gangue (quartz) material. Reilly (1986) described the distribution of “molybdenum mineralisation” on the 1400 feet level of Mountain Mine, associated with high-grade copper mineralisation. Zones with a “cherty” appearance of quartz were identified as “dust-like” grains of molybdenite and pyrite (Fletcher 1969). Selenium and tellurium minerals, as well as molybdenum and traces of gold, silver and mercury have been identified from the Allihies Mines (Reilly 1986; Spinks *et al.* 2016).

Previous microthermometry measurements of syn-Variscan quartz veins from Mizen Peninsula suggest peak-metamorphic conditions of between 300-400 °C (Wen *et al.* 1996). Detailed fluid inclusion studies from Allihies (near Mountain Mine) by Meere and Banks (1997) indicate medium to moderate salinities (4-16 wt% $NaCl_{equiv}$) for syn-Variscan quartz veins and high salinities (22-27 wt% $NaCl_{equiv}$) for post-orogenic extensional veins. At Hungry Hill (about 19 km ENE of Allihies) Rogers (2002) compared early veins (T_h = 230 °C) with the syn-buckling veins (syn-Variscan, T_h = 190 °C) and late stage veins (T_h = 170 °C). All 3 vein types have a moderate salinity of about 10 wt% $NaCl_{equiv}$.

Methodology

Field mapping focussed primarily on the classification, measuring and sampling of quartz veins to establish a paragenesis and a structural chronology. Aerial drone mapping was utilised to investigate the area around the Allihies copper mines and to contextualise features identified in the field. A DJI Phantom 3 Professional with a 4K, 12.4-megapixel camera was flown at a vertical height of between 20 to 50 m, depending on the surface topography, over a defined area of approximately 30,000 m^2 per flight. Several flights were necessary to cover the entire mining area (Fig. 3a). The high-resolution images were captured with two thirds overlap. The geotagged images were processed with the photogrammetry software 3Dsurvey by Modri planet to calculate a 3-dimensional (3-D) digital terrain model (DTM) and a 2-D high-resolution orthorectified photograph, subsequently georeferenced in ArcGIS (Fig. 3a). The high-resolution drone orthophotography and aerial photography aided the field mapping of the faults and veins. The low capturing elevation facilitated the identification of veins and structures as small as 6 cm wide.

The 3-D DTM point cloud and historical mining maps (Wilson & Powell 1956) were used to create a 3-D model of Mountain Mine and its mineralised veins (see digital appendix). Data entry and 3-D modelling was done using SKUA-GoCAD (Emerson Paradigm) and the Mining Suite plugins of Mira Geoscience, using the discrete smooth interpolator to model the veins (Caumon *et al.* 2009). Data entry and georeferencing was performed in ArcMap (ESRI). Data validation and visualization were carried out with Leapfrog3DGeo (ARANZ Geo Ltd., now Seequent).

Sampling of mineralised and unmineralised quartz veins was conducted in the entire area around Allihies. Whenever possible, in-situ vein samples were taken, but in some cases the historic mine shafts were not accessible, collapsed or filled with water. This necessitated the collection and analysis of some samples from spoil material.

The samples were petrographically analysed as polished blocks and polished thin sections via reflected and transmitted light microscopy. Images were captured using a Leica (DVM2500) digital microscope with an attached VZ700C lens in the Geomicroscopy Facility at University College Cork.

Four spatially oriented samples from East-West striking mineralised quartz veins were collected and cut perpendicularly to cleavage $S_{1,vein}$ (sample 418; Fig. 3a). Thin section images were captured and stitched for the entire width of the veins with the Leica DVM2500 digital microscope as false colour images to identify different generations and microstructures.

All vein types were prepared as doubly polished thin sections. Small chips of max. 1cm^2 were examined with a Linkam (LMS600) temperature-controlled microscope stage, combined with an Olympus BX50 microscope, a x100 LWD objective and an attached 16 megapixels Nikon DS-Ri2 camera at the UCC Geomicroscopy Facility. Bi-phase (L+V) fluid inclusions, were analysed for their freezing temperature T_{ice}, the first melt temperature T_{fm} and the final melt temperatures T_m, as well as the homogenisation temperature T_h = liquid + vapour = liquid. Special care was taken to measure primary fluid inclusion assemblages. Secondary inclusion trails and healed areas were avoided. Within the mineralised veins, primary inclusions were selected, which are genetically related to the copper sulphides. The stage was calibrated using a CO_2 standard (-56.6 °C, Camperio) and a synthetic, doubly distilled H_2O standard (T_m = 0.0 °C, T_h = L + V = L: 374.0 °C, Leoben). Salinity was calculated as wt% $NaCl_{equiv}$ by using the Excel macro HOKIEFLINCS_H2O-NACL (Steele-MacInnis *et al.* 2012; Bodnar 1993; Atkinson 2002; Bodnar *et al.* 1994; Bodnar 1983).

A historic molybdenite sample (BM.1964,R231) from Mountain Mine (Fig. 2) was provided by the National History Museum in London (NHM). The mineralised quartz-molybdenite specimen was collected by Sir Arthur Russell from the Mountain Mine dumps in 1918 (NHM Russell collection). A second molybdenite sample was discovered recently from spoil near Caminches Mine (Fig. 2). Small fragments (< 1 cm) were separated from the samples using a micro chisel to avoid major damage and potential rhenium contamination. The samples, which both contain fine-grained molybdenite (< 2 mm), were analysed using reflected light microscopy and fluid inclusion microthermometry (quartz). The samples were used for Re-Os geochronology at Durham University Laboratory for Source Rock and Sulfide Geochemistry and Geochronology. Sample preparation and analysis was undertaken as described in detail by Selby & Creaser (2001) and Li *et al.* (2017). The molybdenite material was isolated from the vein quartz and other minerals with HF. Approximately 10mg of pure molybdenite was loaded into a carius tube with aqua regia (3 ml HCl + 6 ml HNO_3) and a known about of tracer solution (^{185}Re + isotopically normal Os). The carius tube was then sealed and placed in an oven for 24 hrs at 220˚C. The Os and Re isotopically equilibrated sample and tracer solution were extracted from the acid solution using solvent extraction, microdistillation and anion chromatography methods. The purified Re and Os fractions were measured for their isotopic compositions in static mode using a Thermo Scientific Triton mass spectrometer in the Arthur Holmes Laboratory at Durham University. The Re-Os molybdenite model age was calculated with the equation $t = \ln(^{187}Os/^{187}Re + 1)/\lambda$ (Smoliar *et al.* 1996), where λ is the decay constant for ^{187}Re = 1.666×10^{-11} a^{-1} (Smoliar *et al.* 1996; Selby *et al.* 2007). Uncertainties were calculated with mass spectrometry uncertainty, all analytical sources uncertainties and the decay constant (Table 1).

Results

<u>Field Observations</u>

Host Lithologies

The area north of Mountain Mine is dominated by micaceous siltstones and quartz arenites of the Allihies Sandstone Member (Caha Mountain Formation). The siltstones have a reddish to greyish colour and form beds from 10 cm to several metres thick. The sandstones are red to grey and are generally well sorted. Occasionally, siltstone clasts up to 2 cm were found within the sandstone. Ripple marks and mud cracks occur on the bedding planes. Grey mudstones of the Ballydonegan Slate Member are mainly observed in the southern part of the study area between Mountain Mine and Allihies village.

Both lithologies can display alteration zones adjacent to large (> 0.5 m width) mineralised quartz veins. The colour varies from yellowish-brown to pale yellowish-red, mainly due to the presence of iron hydroxides. These alteration zones are rarely wider than one metre around the mineralised veins but next to the smaller veins (< 10 cm width) they are often absent.

Early extensional structures and mineralisation

East-West striking, normal faults with a strike-length of 60 to over 1000 m are present near, and at, the historic mine shafts (Fig. 3a). Their strike ranges in between 071 and 123 degrees. Due to surface weathering, these faults form natural depressions. Figure 3b shows a quartz vein following a steep dipping (70 degrees) normal E-W striking fault SW of Mountain Mine (Fig. 3a). This vein is deformed by a subsequent orogenic compression.

Sub-parallel to ESE-WNW striking quartz veins occur up to 35 m from the E-W faults (Fig. 3a and Fig. 4a). These veins are mineralised and range from centimetre to metre scale in diameter and have a maximum length of over 100 m. Only two vein sets have been observed striking North-South, including the N-S Lode at Mountain Mine (Fig. 3a).

Associated with larger quartz veins are a spatially concentrated series of smaller quartz veinlets with an average width of 0.5 to 10 cm and a maximum length of 108 m (Fig. 3a). Similar to the larger veins and lodes, these smaller veins have an ESE-WNW strike with a nearly vertical dip (Fig. 4b). Major mineral constituents are quartz, fine disseminated chlorite and minor amounts of chalcopyrite.

Figure 5 (and Dig. App.) displays the extent of the underground workings at Mountain Mine, where it is evident that the E-W Lode and the New E-W Lode are connected by the N-S Lode. It is important to note that the E-W Lode extends to the West of N-S Lode while the New E-W Lode extends to the East of N-S Lode. Both extensions pinch out laterally.

In places, sets of multiple sub-parallel and closely spaced veins form lodes with a maximum surface outcrop of up to 18 m in width and up to 160 m in length (Fig. 6). The Marion Lode (Fig. 3a and Fig. 6) is formed by multiple generations (G1-G3) of E-W striking mineralised and brecciated quartz (G1), mineralised quartz (G2) and sub-horizontal unmineralised thinner quartz (G3). Corrugations on the vein wall of (G1) and rotated vein fragments indicate strike slip movement parallel to the vein orientation (Fig. 6).

Mineralisation of the large orebodies is dominated by chalcopyrite with minor amounts of bornite and late veinlets of tetrahedrite/tennantite. Aggregates of fine-grained chlorite and late cavity-fill siderite with minor calcite, associated with malachite were found on spoil material from Caminches Mine (Fig. 2). Pockets of clear, vuggy quartz crystals (up to 2 cm) are present in the outcrop of the massive Coom Lode.

At the surface, most of the lodes and the smaller E-W veins do not show any evidence of copper mineralisation. Malachite staining occurs only at fresh outcrops of the historical mines. Due to the lack of free carbonate within the sediments, malachite can be completely absent. Traces of reddish goethite staining, as well as extensively altered chalcopyrite can be found about 20 to 40 cm below the surface within the veins. Apparently barren, but mineralised veins were identified by the presence of epimorphs caused by weathered sulphides and the internal reddish staining from iron hydroxides, often visible through the partially translucent quartz as pale red staining.

Syn-Compressional structures

Large scale SW-NE trending faults cut the sedimentary succession into elongate blocks up to 550 m lateral length, and result in predominantly sinistral offset of the E-W faults with a maximum dislocation of 17 m observed near the New E-W Lode (Fig. 7a). SE-NW to SSE-NNW striking faults (e.g. Cornish Village Fault, Fig. 2 and Fig. 7a) constrain northern and southern boundaries of the fault blocks. All ESE-WNW trending veins are affected by oblique faulting with lateral sinistral offsets of up to 83 m (Fig. 7b and Fig. 7c).

Thin beds (max. 30 cm) of the competent sandstones were found boudinaged in between layers of less competent siltstones. Penetrative cleavage is clearly visible within the siltstones, but less distinctive within the sandstones. The cleavage in the slates has a phyllitic texture and a high amount of sericitic, fine crystalline mica. Cleavage $S_{1,\ host}$ has a general SW-NE strike with a sub-vertical dip (Fig. 4c). Some of the early quartz veins (e.g. at Great Mountain Mine North and Coom Mine, Fig. 7b and Fig. 7c) show clear evidence of syn-compressional cleavage development (Fig. 8a), S_1 cleavage-refraction in the veins compared to the surrounding siltstones (Fig. 8b) and cataclastic deformation (Fig. 8c). Smaller E-W veins sometimes display asymmetric folding, cleavage and boudinage.

Second and third order step folds show bedding-S_1-cleavage intersection lineations with a mean plunge of 47 degrees to the southwest (N = 55, Fig. 4d). These folds have an asymmetrical step geometry with limbs dipping from the northwest to the southeast with a shallow to vertical angle (Fig. 4e). Metre-scale joints observed are generally oriented SE-NW with a sub-vertical dip (Fig. 4f).

Other compressional structures (Fig. 3b) include saddle reef quartz veins up to one metre wide and 10 cm thick (Fig. 8d), and en echelon quartz tension gash arrays in semi-brittle shear zones ranging from 40 cm to several metres in length. These vein types host disseminated chlorite, as well as aggregates of chlorite. Subvertical extension related to subsequent tectonic compression led to the development of shallow dipping quartz veins within the earlier extensional lodes.

Vein petrography and microstructures

Early extensional E-W veins

Combined reflected and transmitted light microscopy show a coeval paragenesis of elongate blocky quartz and chalcopyrite mineralisation within veins (Mountain Mine, Fig. 9a). Quartz grains with cogenetic chalcopyrite and bornite with chalcopyrite exsolution lamellae were found in a sample from Mountain Mine spoil. Both minerals are partially surrounded by chalcocite of the same generation. Alteration seams with blue covellite and goethite occur around the sulphides as a result of supergene alteration. Parts of the mineralised veins are cross-cut by later quartz veinlets. Some specimens from Mountain Mine (Gunpowder Mine, Fig. 3a) contain quartz-chalcopyrite-tetrahedrite/tennantite veins, which are cross-cut by later tetrahedrite/tennantite-quartz-chalcopyrite veinlets. Minor amounts of specular hematite occur within a sample from Coom Lode (Fig. 2). Reflected light microscopy on the historic molybdenite material from Mountain Mine (BM.1964,R231) indicate a syngenetic intergrowth of quartz, molybdenite and minor chalcopyrite (Fig. 9b). Figure 9c shows the generalised paragenetic sequence of the E-W veins with all minerals observed in this study at the different mines of the Allihies District.

Syn-Compressional veins

The syn-compressional veins are mainly formed by stretched (Bons *et al.* 2012) to fibrous quartz crystals with sweeping type to no undulous extinction (Trouw *et al.* 2009). The fibrous quartz crystals are perpendicular to the vein walls but can be curved within the vein itself. As there are no clearly visible median zones, these veins are dominated by antitaxial crystal growth (Bons *et al.* 2012).

Compressional deformation of E-W veins

Microstructural examination of oriented, mineralised, E-W striking quartz veins (Sample 418, Fig. 3a) show a predominance of syntaxial elongate blocky quartz crystals (Fig. 9a and Fig. 10, Sample 418_A). The larger crystals in the vein centre have no or sweeping type undulous extinction with lobate contacts due to grain boundary migration (Trouw *et al.* 2009). The smaller crystals at the margin with the host-rock show patchy undulous extinction (Trouw *et al.* 2009). WSW to ENE striking, intergranular secondary fluid inclusion trails occur in sample 418_B2 (Fig. 10). Vein samples 418_B1 and 418_B3 (Fig. 10) show centimetre wide, E-W striking cataclastic zones with anhedral and subhedral microcrystals in between the elongate blocky areas. In the case of vein B3, these cataclastic zones are associated with microfractures. Similar to vein A, the smaller crystals in vein B show a patchy undulous extinction, while the larger elongate blocky crystals show sweeping extinction and have lobate contacts. Sample 418_B1 (Fig. 10) shows en echelon microveins with sinistral movement indicators along E-W strikes. In vein 418_B3 intensive brecciation of the elongate blocky crystals is visible with fine grained zones of subhedral crystals and cataclastic seams around microfractures (Fig. 10, vein B3 magnified images).

Fluid inclusion microthermometry

Fluid inclusions were measured on mineralised lodes and smaller E-W veins, as well as syn-compressional (saddle reef and en echelon) vein samples.

Extensional E-W veins

Fluid inclusions in the mineralised, quartz veins, including the historic molybdenite sample, are generally oval shaped and consist of an undersaturated liquid-rich phase, and a vapour phase between 0.5 and 15 volume percent. Homogenisation temperatures T_h range between 121 and 272 °C (Fig. 11a). The salinities vary between 3.2 and 25.4 wt% $NaCl_{equiv}$. Fluid inclusions from the later tetrahedrite/tennantite-quartz-chalcopyrite veinlet show higher homogenisation temperatures with a maximum of 314 °C and a mean salinity of 15.5 wt% $NaCl_{equiv}$ (n = 9). Some of the fluid inclusions from this veinlet decrepitated at temperatures from around 259 °C. The pockets of vuggy, clear quartz from the Coom lode, which indicate a late formation of the early extensional veins contain unaltered, primary fluid inclusions up to 60 µm and display a very high salinity of up to 28.5 wt% $NaCl_{equiv}$ and low homogenisation temperatures with a minimum of 74 °C (Fig. 11a).

Overall, the fluids of the E-W mineralised, quartz veins range from moderate salinity and high homogenisation temperatures to high salinities and very low homogenisation temperatures. Similar trends are observed in the small E-W veins which are associated with the mineralised veins (Fig. 3a, Fig. 8b and Fig. 11a).

The eutectic melting $T_{first\ melt}$, which indicates the salinity composition, shows a mode between -24 to -20 °C (Fig. 11b) for the extensional veins.

Syn-compressional veins

The fluid inclusions in the syn-compressional quartz veins are mainly elongate and consist of a liquid and a vapour phase (between 0.5 and 5 vol.%). They have an average size of 10 µm (max. 22 µm) and display homogenisation temperatures ranging between 121 and 243 °C (outlier: 309 °C), and low to moderate salinities between 8.2 and 19.1 wt% $NaCl_{equiv}$ (Fig. 11a).

The eutectic melting $T_{first\ melt}$ of the compressional veins show a mode of temperatures between -18 and -14 °C (Fig. 11b).

Re-Os molybdenite geochronology

The fine grained (grain size < 2 mm) molybdenite sample from Mountain Mine spoil (BM.1964,R231, Fig. 9b) possesses 43.9 ± 0.2 ppm Re, 27.6 ± 0.1 ppm ^{187}Re and 169.1 ± 0.8 ppb ^{187}Os. The ^{187}Re-^{187}Os data yield to a model age of 366.4 ± 1.9 Ma for the molybdenite mineralisation. The molybdenite sample from Caminches Mine spoil is also fine grained and has 3.83 ± 0.04 ppm Re, 2.41 ± 0.03 ppm ^{187}Re and 14.78 ± 0.16 ppb ^{187}Os. The ^{187}Re-^{187}Os model age is 367.3 ± 5.5 Ma.

Table 1. *Re-Os isotope data and model ages for the molybdenite samples from Allihies Mountain Mine (BM.1964,R231) and Caminches Mine (Fig. 2).*

Discussion

Large E-W faults, such as the Coomnacronia-Killarney-Mallow Fault Zone and the Cork-Kenmare Fault Zone (Fig. 1, Naylor & Jones 1967; Capewell 1975; Price & Todd 1988; Meere 1995; Vermeulen *et al.* 2000; Landes *et al.* 2003; MacCarthy 2007; Ennis *et al.* 2015) played an important role in the development of the Munster Basin. These major faults are part of a southwards progressing extensional fault system (Landes *et al.* 2003). Mineralised vein systems follow the same strike as these basin controlling structures (Fig. 12a). The E-W faults would have acted as pathways for the mineralising fluids.

Recent sulphur isotope studies on chalcopyrite from the Allihies Mining Area (Spinks *et al.* 2016) show consistent negative $\delta^{34}S$ values (-16.9 to -10.4 ‰). These values imply a biogenic sedimentary origin. This could indicate copper remobilisation from the host sediments into the quartz veins. Another possibility would be a more distant copper source. Meere & Banks (1997) described a basinal sediment infill of over 6 km. As the pre-Variscan, extensional E-W faults can be laterally extensive (e.g. Williams 2000; Landes *et al.* 2003; MacCarthy 2007; Ennis *et al.* 2015; Fig. 1), it is possible, that their extension to depth can reach the basement. According to seismic interpretation from Landes *et al.* (2003) a P-wave velocity change in 13 – 14 km depth possibly indicates the termination of the basin controlling, E-W striking Cork-Kenmare Fault Zone (Fig. 1). This suggests that some of the major extensional fault zones extend below the basin infill.

The 3D model (Fig. 5) displaying the historic underground workings shows that the North-South Lode connects to the East-West Lode and the New East-West Lode at Mountain Mine. Previous workers described this arrangement as a Z-shaped structure of the Mountain Mine Lodes (e.g. Fletcher 1969; Reilly 1986). This is a misleading description, as both the E-W striking lodes extend laterally beyond the N-S Lode before pinching out (Fig. 3a and Fig. 5) This structure could be interpreted as a transfer fault or breached relay ramp (Walsh & Watterson 1991; Fossen & Rotevatn 2016) that developed during the early extensional phase.

The smaller E-W striking quartz veins appear to be barren at the surface. Their classification was only possible with the help of the drone and satellite imaging as it is clearly visible on Figure 3a, that the smaller E-W striking veins are always aligned parallel to the larger mineralised lodes. It seems that the smaller E-W veins are branches of larger lodes in their immediate proximity. According to this, the smaller E-W veins and the mineralised lodes can be classified together as pre-Variscan early extensional veins. Due to extensive surficial leaching processes mineralised quartz veins could be misinterpreted as barren. Reilly (1986) already mentioned this “apparently barren nature of the outer metre or so” at the Mountain Mine Lodes.

Meere & Banks (1997) sampled an extensional quartz vein (Fig. 3b) near Mountain Mine that showed high salinities (Vein 7, 22-27 wt% $NaCl_{equiv}$) and was identified as a post-orogenic extensional vein. For this study, the identical vein from this locality was sampled again and is now classified as an early extensional vein (Fig. 11a). The pre-Variscan veins cover a quite large field of higher homogenisation temperatures (up to T_h = 271 °C, Fig. 11a) and low salinities (as low as 3.2 wt% $NaCl_{equiv}$), to very low homogenisation temperatures with a minimum of 74 °C and a high salinity of up to 28.5 wt% $NaCl_{equiv}$. The wide range in T_h and salinity, as well as the observed cross-cutting veins (Fig. 6) is interpreted to reflect the complexity of the mineralising fluids which occurred probably in several pulses with variable degrees of end-member fluids that show a spatial and temporal variability. A late cavity fill of vuggy quartz crystals at Coom Mine (Fig. 2 and Fig. 11a) was generated by progressive fluid cooling and an increase in salinity concentration at the end of the early vein filling processes. This development could be very localised, as the vuggy quartz occurs in small pockets within the massive Coom Lode.

The eutectic melting $T_{first\ melt}$ of the early extensional veins is primarily between -24 and -20 °C (Fig. 11b). These measurements which are partially lower than the eutectic melting of -21.1 °C in the H_2O-NaCl system indicate an additional phase. As there is an occurrence of late siderite and minor calcite within the early extensional veins, it could be possible, that minor amounts of $CaCl_2$ was also present during the early mineralisation. This would define a ternary system of H_2O-NaCl-$CaCl_2$ (e.g. Steele-MacInnis *et al.* 2011). Spinks *et al.* (2016) described barite as a further gangue mineral within the mineralised veins which could result as a $BaCl_2$ phase within the fluid system. Nevertheless, no significant amounts of barite were found at the Allihies region during this study. Meere & Banks 1997 showed a high Br/Cl ratio from the Allihies quartz veins, implying an early marine brine signature.

The early E-W veins contain mainly oval shaped inclusions, which is interpreted to demonstrate uniform crystal growth. The shape of the fluid inclusions can be a diagnostic feature in comparison to later compressional quartz veins which show a majority of elongated fluid inclusions. This elongation is probably caused by fibrous crystal growth in the Variscan quartz veins.

Due to their high competency, the East-West striking lodes and large quartz veins apparently cross-cut structures, such as bedding, folding and even faulting. These veins, with a width of at least 40 cm, show only very weak or no folding and the compressional features, caused by the Variscan Orogeny, such as tectonic cleavage and folding (e.g. Cooper & Trayner 1986; Ford 1987) can be easily missed and might be a reason why some previous workers (Sheridan 1964; Halliday & Mitchell 1983; Wen *et al.* 1996; Meere & Banks 1997; Spinks *et al.* 2016) interpreted the timing of the mineralised lodes as a syn- to post-Variscan. Variscan compression (Ford 1987) affected the early mineralised veins and is clearly demonstrated by an intensely cleaved lode ($S_{1,\ vein}$) at Great Mountain Mine (Fig. 8a), or the cataclastic deformation in the Coom Lode (Fig. 8c). Sanderson (1984) identified N-S trending veins on Beara Peninsula as early extension veins with cleavage and mineralisation. The early extensional N-S and NW-SE trending veins seem to be more affected by the syn-Variscan compression than the majority of the E-W trending veins due to the low angle of the vein's strike to the Variscan NNW-SSE maximum principle stress σ_1 (Fig. 7b and Fig. 8a). Smaller E-W veins display a well-developed Variscan cleavage (Fig. 8b) and associated minor folding.

Sinistral faulting of the Great Mountain Mine Lode (Fig. 7b) and the Coom Lode (Fig. 7c) is also interpreted to be a result of NNW to SSE oriented Variscan compression. Minor sinistral faulting of the E-W Lode of Mountain Mine has been described by Matthews (1964) and Reilly (1986) on the 1400 level.

The saddle reef veins (Fig. 8d) are clearly syn-compressional structures and were already described by several authors as syn-Variscan features (e.g. Dolan 1984). A similar genesis is proposed for the en echelon tension gash arrays which are vertical and related to minor shears resulting from the main deformation (Coller 1984). The sub-horizontal veinlets (Fig. 6 generation 3) which are present at Marion Lode and cross-cut all previous vein generations are similar to the sub-horizontal veins (from near Mountain Mine) described by Meere (1995) and are also related to ongoing Variscan compression and associated vertical extension.

Variscan deformation of the early E-W veins has also been identified in the microstructures (Fig. 10). The elongate blocky syntaxial veins, belonging to the early extensional structures (mineralising event, Fig. 10, vein 418_A), were later deformed and developed cataclastic zones, microfractures (Fig. 10, vein 418_B1 and 418_B3) and micro en echelon veins (vein 418_B2). Sweeping undulosity in larger blocky crystals, with lobate contacts in the vein centre and patchy undulosity in the small grains along the vein rim, indicate a low temperature crystal-plastic deformation (Trouw *et al.* 2009). This is in agreement with Meere (1995) who identified a micro brecciated zone within a sample from nearby Mountain Mine as a result of Variscan compression normal to the vein wall. The micro fractures with the seams of cataclastic sub-hedral grains show patchy undulous extinction (Fig. 10 vein B3) and could be explained by deformation under low-grade sub-greenschist facies metamorphism during the Variscan Orogeny (Meere 1995). This provided conditions for a semi-brittle deformation, which caused partially recrystallization and fracturing.

Wen *et al.* (1996) collected syn-Variscan fluid inclusion measurements from Mizen Head with peak temperatures T_h of 300 to 400 °C. These are much higher than the results presented here with approximately 150 to 240 °C for the syn-Variscan quartz veins (Fig. 11a). A possible reason could be the different burial depths between the two locations. Meere & Banks' (1997) results of moderate salinities of 4 to 16 wt% $NaCl_{equiv}$ for syn-Variscan quartz veins fit very well with this study's results of about 8 to 19 wt% $NaCl_{equiv.}$

The eutectic melting $T_{first\ melt}$ of the Variscan veins (-18 to -14 °C, Fig. 11b) is above the eutectic point of the H_2O-NaCl binary system (-21.1 °C). The H_2O-NaCl phases are still the most possible components, as initial melting at the eutectic point of -21.1 °C are difficult to identify, especially at medium to low salinity concentrations. The characteristic shape of the syn-Variscan fluid inclusions is elongated with a high eccentricity.

Following the new vein classification of pre-Variscan early extensional veins and syn-Variscan veins, a simplified genetic model of mineralisation at Allihies is proposed (Figure 12). North-South extension during the development of the Munster Basin and South Munster Basin during the Middle Devonian to early Upper Devonian generated large scale E-W striking extensional faults which provided deep fluid pathways for medium to high saline copper-rich fluids (Fig. 12a). These fluids formed the mineralised, mainly E-W striking, and steep dipping quartz veins seen in the Allihies region.

The relatively high homogenisation temperatures recorded from fluid inclusions during this study with T_h values of up to 314 °C confirm the identification of high geothermal gradients during basin formation (Meere 1995; Williams 2000). This is caused by extensive rifting processes with crustal thinning and resultant upwelling of the Moho (Williams 2000). According to seismic interpretations (Landes *et al.* 2003) the depth of the Moho can vary between 28 and 33 km. The large amount of basinal infill (Meere & Banks 1997) probably provided an excess of pore fluids which could have led to the extensive quartz vein formation.

The end Carboniferous Variscan Orogeny folded and faulted the basin structures generating silica-rich fluids which precipitated quartz veins into tension gashes such as saddle reefs, en echelon veins and sub-horizontal veins (Fig. 12b).

Timing of the copper mineralisation

Based on Pb/Pb model age measurements on vein hosted copper deposits from Ross Island (Killarney, Kerry), Kinnaird *et al.* (2002) assumed a syn-Variscan vein mineralisation between 290 and 270 Ma for the Munster Basin deposits. K-Ar dates (Halliday and Mitchell 1983) from clay minerals which were sampled in Allihies from the wall rock next to the quartz veins produced ages of 290 to 261 Ma for the Mountain Mine Lode and an older age of 321 Ma for an apparently un-mineralised quartz vein. The post-Variscan dates from Allihies are probably caused by a younger alteration of the clay minerals.

The new model, presented in this paper, is supported by molybdenite Re-Os model ages of 367.3 ± 5.5 to 366.4 ± 1.9 Ma (Table 1). It can be assumed that molybdenite formation was contemporaneous with the major copper mineralisation phase based on the petrographical association of molybdenite and chalcopyrite (Fig. 9b) and Reilly's (1986) description of "Molybdenum Mineralization" within the centre of the Main E-W Lode at Mountain Mine.

The Re-Os ages belong to the Famennian Stage (Cohen *et al.* 2019) of the Upper Devonian, suggesting that mineralisation was emplaced during basin development and sedimentation which occurred between the Upper Devonian and Lower Carboniferous (MacCarthy 2007). As no visible disseminated copper is known around the Allihies mining area, partial lithification may have already occurred in the adjacent host sediments to provide an impermeable, barrier to the mineralising fluids. On the other hand, all sedimentary copper could have been remobilised into the quartz veins and the sedimentary source was therefore older than the vein mineralisation. This would explain the sedimentary sulphur isotope signature described by Spinks *et al.* (2016). The lamprophyric intrusions at Black Ball Head (314.44 ± 1.00 Ma, Quinn *et al.* 2005), dated as coinciding with the Variscan compression (Sanderson 1984; Ford 1987; Meere 1995) postdate the mineralisation.

This new model puts the copper mineralisation at Allihies into a similar tectonic setting as the formation of large Zn-Pb deposits at Navan, Lisheen (pyrite Re-Os 346.6 ± 3.0 Ma, Hnatyshin *et al.* 2015) in the Lower Carboniferous to the north. Similar to this study, the well investigated Zn-Pb deposits, such as Silvermines (334.0 ± 6.1 Ma, Hnatyshin *et al.* 2015) and Tynagh Mine (Irish Midlands, e.g. Kinnaird *et al.* 2002), are related to E-W striking faults, caused by a pre-Variscan North-South extensional phase (e.g. Hitzman 1999). Comparable to Allihies, the Variscan compression of the Irish Midlands deposits had only little effect on mineralisation related normal faults of these deposits (Hitzman 1999). Further similarities can be observed with fluid inclusion salinities and homogenisation temperatures (Fig. 11a). Comparable to the pre-Variscan extensional veins from the Allihies District, the Irish Type Deposits show a range of homogenisation temperatures T_h up to about 240 °C and low salinities (about 10 wt% $NaCl_{equiv}$), to very low homogenisation temperatures with a minimum of about 55 °C and a high salinity of up to 24 wt% $NaCl_{equiv}$ (Wilkinson 2001; Wilkinson 2010; Gleeson & Yardley 2002).

Conclusions

The Allihies Mining District is dominated by two different quartz veining generations:

(1) Quartz veins with a general E-W strike are associated with early-extensional faults and branch out to smaller E-W striking veins. These veins bear the primary copper mineralisation as mainly chalcopyrite, bornite, tetrahedrite/tennantite and molybdenite. The timing of the mineralisation is dated by molybdenite Re-Os geochronology of 367.3 ± 5.5 to 366.4 ± 1.9 Ma. The dates coincide with basin development and shortly post-date the early sedimentation sequences during the Upper Devonian. These appear to be directly related to large, basin controlling E-W faults.
Fluid inclusion data suggest moderate to high salinity with homogenisation temperatures of up to 314 °C. Eutectic melting indicates a ternary fluid system.

(2) Syn-Variscan veins occur as saddle reefs and en echelon tension gash shear structures. Sub-horizontal veins cross-cut early extensional structures.
The homogenisation temperature is around 200 °C with moderate salinities.

Drone imaging and aerial photograph interpretation has proven to be very beneficial for the identification of pre-compressional features at the Allihies Mining District.

Acknowledgements

This publication has emanated from research supported in part by a research grant from Science Foundation Ireland (SFI) under Grant Number 13/RC/2092 and is co-funded under the European Regional Development Fund and by iCRAG industry partners.

SCJ is supported by iCRAG under the Science Foundation Ireland, EU Regional Development Fund and industry partners (13/RC/2092), as well as SFI research grant 16/RP/3849.

The work of KT was funded from the European Union’s Horizon 2020 research and innovation program under Marie Skłodowska-Curie grant agreement no. 745945.

The authors are grateful for the assistance from Lingli Zhou (Trinity College Dublin) for the precise geochemical classification of the tennantite/tetrahedrite mineralisation. Many thanks to David van Acken (University College Dublin) for the initial geochronology on chalcopyrite which lead to the new perspective and finally to the new discoveries presented in this publication. Thanks to Tadhg O'Sullivan and his colleagues from the Allihies Copper Mine Museum for the historical background knowledge and granting access to the underground workings of Allihies Mountain Mine. Many thanks to Geoff Long (University of Portsmouth) for his support with thin section preparation. Special thanks to the National History Museum in London (Simon Kocher and Robin Hansen) for providing molybdenite sample material (BM.1964,R231) from the historic Russell collection. Thanks to Kate Kiseeva for providing her recent finding of molybdenite from Caminches Mine.

The Geological Survey Ireland are acknowledged for providing regional data and background information for our 2-D mapping and 3-D modelling efforts. We also thank ARANZGeo/Seequent (Leapfrog3DGeo), Emerson Paradigm (SKUA-GoCAD), Microsoft (Bing Satellite Maps), Mira Geoscience (Mining Suite Plugins), Modri planet d.o.o. (3Dsurvey) and ESRI (ArcGIS) for providing support and academic licenses of software essential to this project.

DS acknowledges the technical support of Antonia Hoffman, Geoff Nowell and Chris Ottley, and the Total Endowment Fund and the CUG Wuhan Dida Fund.

Thanks also to the reviewers Samuel C. Spinks and Eddie Dempsey, as well as to the editor John MacDonald who commented on the earlier version of this manuscript and helped to improve this paper.

References

Allmendinger RW, Cardozo NC, Fisher D (2013) Structural Geology Algorithms: Vectors & Tensors: Cambridge, England. Cambridge University Press, 289 pp

Atkinson AB Jr. (2002) A Model for the PTX Properties of H2O-NaCl. Unpublished MSc Thesis, Dept. of Geosciences, Virginia Tech, Blacksburg VA, 133 pp

Blenkinsop HG (1902) Notes on the Berehaven copper mines. Trans. Inst. Mining and Metall 12: 1-7

Bodnar RJ (1983) A method of calculating fluid inclusions volumes based on vapor bubble diameters and P-V-T-X properties of inclusion fluids. Economic Geology 78: 535-542

Bodnar RJ (1993) Revised equation and table for determining the freezing point depression of H2O-NaCl solutions. Geochimica et Cosmochimica Acta, 57: 683-684

Bodnar RJ, Vityk MO (1994) Interpretation of microthermometric data for H2O-NaCl fluid inclusions. In: De Vivo B, Frezzotti ML (eds) Fluid Inclusions in Minerals, Methods and Applications. Virginia Tech, Blacksburg, VA, pp 117-130

Bons PD, Elburg M, Gomez-Rivas E. (2012) A review of the formation of tectonic veins and their microstructures. Journal of Structural Geology 43: 33-62

Capewell J (1975) The Old Red Sandstone Group of Iveragh, Co. Kerry. Proceedings of the Royal Irish Academy. Section B: Biological, Geological, and Chemical Science 75: 155-171

Cardozo N, Allmendinger RW (2013) Spherical projections with OSXStereonet. Computers & Geosciences 51(0): 193-205

Caumon G, Collon-Drouaillet P, Le Carlier de Veslud C, Viseur S, Sausse J (2009) Surface-based 3-D modeling of geological structures. Mathematical Geosciences 41: 927–945.

Cohen KM, Harper DAT, Gibbard PL (2019) ICS International Chronostratigraphic Chart 2019/05. International Commission on Stratigraphy, IUGS. www.stratigraphy.org. Accessed 12 August 2019

Coller DW (1984) Variscan structures in the Upper Palaeozoic rocks of west central Ireland. Geological Society, London, Special Publications 14(1): 185-194

Cooper MA, Trayner PM (1986) Thrust-surface geometry: implications for thrust-belt evolution and section-balancing techniques. Journal of Structural Geology 8(3-4): 305-312

Daltry VDC (1985) A structural, geochemical and mineralogical appraisal of the stratabound ore deposits in western County Cork, Ireland. Thesis, University College Cardiff, Wales

Dolan JM (1984) A structural cross-section through the Carboniferous of northwest Kerry. Irish Journal of Earth Sciences, pp 95-108

Ennis M, Meere PA, Timmerman MJ, Sudo M (2015) Post-Acadian sediment recycling in the Devonian Old Red Sandstone of Southern Ireland. Gondwana Research 28(4): 1415-1433

Fletcher CI (1969) The sulphide mineralization in the Allihies region, County Cork, Eire. Dissertation, University of Leicester, pp 128-129

Ford M (1987) Practical application of the sequential balancing technique: an example from the Irish Variscides. Journal of the Geological Society 144(6): 885-891

Fossen H, Rotevatn A (2016) Fault linkage and relay structures in extensional settings - A review. Earth-Science Reviews 154: 14-28

Gleeson SA, Yardley BWD (2002) Extensional Veins and Pb-Zn Mineralisation in Basement Rocks: The Role of Penetration of Formation Brines. In: Stober I, Bucher K (eds) Water-Rock Interaction. Water Science and Technology Library, vol 40. Springer, Dordrecht

Halliday AN, Mitchell JG (1983) K–Ar ages of clay concentrates from Irish orebodies and their bearing on the timing of mineralisation. Earth and Environmental Science Transactions of the Royal Society of Edinburgh 74(1): 1-14

Hitzman MW (1999) Extensional faults that localize Irish syndiagenetic Zn-Pb deposits and their reactivation during Variscan compression. Geological Society, London, Special Publications 155(1): 233-245

Hnatyshin D, Creaser RA, Wilkinson JJ, Gleeson SA (2015) Re-Os dating of pyrite confirms an early diagenetic onset and extended duration of mineralization in the Irish Zn-Pb ore field. Geology 43 (2): 143-146

Jarvis A, Reuter HI, Nelson A, Guevara E (2008) Hole-filled SRTM for the globe Version 4. International Centre for Tropical Agriculture (CIAT). http://srtm.csi.cgiar.org. Accessed 25 July 2017

Kinnaird JA, Ixer RA, Barreiro B, Nex PA (2002) Contrasting sources for lead in Cu-polymetallic and Zn–Pb mineralisation in Ireland: constraints from lead isotopes. Mineral Deposita 37(5): 495-511

Landes M, O'Reilly BM, Readman PW, Shannon PM, Prodehl C (2003) VARNET-96: three-dimensional upper crustal velocity structure of SW Ireland. Geophysical Journal International 153(2): 424-442

Li Y, Selby D, Condon D, Tapster S (2017) Cyclic Magmatic-Hydrothermal Evolution in Porphyry Systems: High-Precision U-Pb and Re-Os Geochronology Constraints on the Tibetan Qulong Porphyry Cu-Mo Deposit. Economic Geology 112 (6): 1419-1440

MacCarthy IAJ (1990) Alluvial sedimentation patterns in the Munster Basin, Ireland. Sedimentology 37: 685-712

MacCarthy IAJ (2007) The South Munster Basin of southwest Ireland. Journal of Maps 3:1: 149-172

MacCarthy IAJ, Pracht M, Sleeman AG (2002) Geology of West Cork, Scale 1:100000, Sheet 24. Geological Survey of Ireland

Matthews PFP (1964) The Copper Mineralization near Allihies, Co. Cork. Dissertation, Trinity College, Dublin

Meere PA (1995) High and low density fluids in a quartz vein from the Irish Variscides. Journal of Structural Geology 17(3): 435-446

Meere PA (1995) Sub-greenschist facies metamorphism from the Variscides of SW Ireland an early syn-extensional peak thermal event. Journal of the Geological Society 152(3): 511-521

Meere PA (1995) The structural evolution of the western Irish Variscides: an example of obstacle tectonics? Tectonophysics 246(1-3): 97-112

Meere PA, Banks DA (1997) Upper crustal fluid migration: an example from the Variscides of SW Ireland. Journal of the Geological Society 154(6): 975-985

Naylor D, Jones PC (1967) Sedimentation and tectonic setting of the Old Red Sandstone of southwest Ireland. In: Oswald D (ed) International Symposium on the Devonian System (Calgary), Alberta. Soc. Petrol. Geol. 2: 1089-1099

O'Brien MV (1959) The future of non-ferrous mining in Ireland. In: The future of Non-Ferrous Mining in Great Britain and Ireland. Inst. Mining and Metallurgy Symposium

O'Brien WF (1987) The dating of the Mt Gabriel-type copper mines of West Cork. Journal of the Cork Historical and Archaeological Society 92: 50-70

Pracht M (2000) Controls on magmatism in the Munster Basin, SW Ireland. Geological Society, London, Special Publications 180(1): 303-317

Pracht M, Sleeman AG (2002) A geological description of West Cork and adjacent parts of Kerry to accompany the Bedrock Geology, 1:100,000 Scale Map Series, Sheet 24, West Cork. With accompanying contributions by Wright G (Groundwater) and Cox W (Minerals), Geological Survey of Ireland, 79 pp

Pracht M, Kinnaird JA (1995) Mineral chemistry of megacrysts and ultramafic nodules from an undersaturated pipe at Black Ball Head, County Cork. Irish Journal of Earth Sciences 47-58

Price CA, Todd SP (1988) A model for the development of the Irish Variscides. Journal of the Geological Society 145(6): 935-939

Quinn D, Meere PA, Wartho JA (2005) A chronology of foreland deformation: Ultra-violet laser 40Ar/39Ar dating of syn/late-orogenic intrusions from the Variscides of southwest Ireland. Journal of Structural Geology 27(8): 1413-1425

Reilly TA (1986) A review of vein mineralization in SW County Cork, Ireland. In: Andrew CJ, Crowe RWA, Finlay S, Pennell WM, Pyne JF (eds) Geology and Genesis of Mineral Deposits in Ireland. Irish Association for Economic Geology, Dublin, pp. 513–544

Rogers JG (2002) Regional veining in the Upper Palaeozoic Munster and South Munster Basins, Ireland; the evolution of palaeofluids and palaeofluid flow during basin inversion. Dissertation, University College Cork, Ireland, 283 pp

Sanderson DJ (1984) Structural variation across the northern margin of the Variscides in NW Europe. Geological Society, London, Special Publications 14(1): 149-165

Selby D, Creaser RA (2001) Re-Os geochronology and systematics in molybdenite from the Endako porphyry molybdenum deposit, British Columbia, Canada. Economic Geology 96: 197-204

Selby D, Creaser RA, Stein HJ, Markey RJ, Hannah JL (2007) Assessment of the 187Re decay constant by cross calibration of Re-Os molybdenite and U-Pb zircon chronometers in magmatic ore systems. Geochimica et Cosmochimica Acta 71: 1999-2013

Sheridan DJ (1964) The structure and mineralisation of the Mountain Mine area, Allihies, west Co. Cork, Ireland. Royal Dublin Society, Series A, 2: 21-27

Smoliar MI, Walker RJ, Morgan JW (1996) Re-Os ages of group IIA, IIIA, IVA, and IVB iron meteorites. Science 271: 1099-1102

Spinks SC, Parnell J, Bellis D, Still J (2016) Remobilization and mineralization of selenium–tellurium in metamorphosed red beds: Evidence from the Munster Basin, Ireland. Ore Geology Reviews 72: 114-127

Steele-MacInnis M, Bodnar RJ, Naden J (2011) Numerical model to determine the composition of H2O–NaCl–CaCl2 fluid inclusions based on microthermometric and microanalytical data. Geochimica et Cosmochimica Acta 75(1): 21-40

Steele-MacInnis M, Lecumberri-Sanchez P, Bodnar RJ (2012) Short note: HokieFlincs_H2O-NaCl: A Microsoft Excel spreadsheet for interpreting microthermometric data from fluid inclusions based on the PVTX properties of H2O-NaCl. Computers & Geosciences 49: 334-337

Stein HJ, Markey RJ, Morgan JW, Hannah JL, Schersten A (2001) The remarkable Re-Os chronometer in molybdenite: How and why it works. Terra Nova 13: 479-486

Trouw RAJ, Passchier CW, Wiersma DJ (2009) Crystal-Plastic Deformation, Recovery and Recrystallisation of Quartz. In: Atlas of Mylonites- and Related Microstructures. Springer, Berlin, Heidelberg: 241-262

Unknown Author (1919) Historic mining map, Allihies Copper Mines. Geological Survey of Ireland, GSI Goldmine. https://secure.dccae.gov.ie/goldmine/docpage.html?id1=8260590&id2=9553634&id3=9556911. Accessed 16 July 2017

Vermeulen NJ, Shannon PM, Masson F, Landes M (2000) Wide-angle seismic control on the development of the Munster Basin, SW Ireland. In: Friend PF, Williams BPJ (eds) New perspectives on the Old Red Sandstone. Geological Society, London, Special Publication 180: 223-237

Walsh JJ, Watterson J (1991) Geometric and kinematic coherence and scale effects in normal fault systems. In: Roberts AM, Yielding G, Freeman B (eds) The Geometry of Normal Faults. Geological Society, London, Special Publication 56: 193-203

Wen N, Boyce AJ, Fallick AE, Ashworth JR, Ixer RA (1996) The genesis of Cu-bearing quartz veins by metamorphic remobilization from stratiform red bed deposits, SW County Cork, Ireland. Mineralogy and Petrology 57(1-2): 73-89

Wilkinson JJ (2001) Fluid inclusions in hydrothermal ore deposits. Lithos 55(1-4): 229-272

Wilkinson JJ (2010) A Review of Fluid Inclusion Constraints on Mineralization in the Irish Ore Field and Implications for the Genesis of Sediment-Hosted Zn-Pb Deposits. Economic Geology 105: 417-442

Williams EA (2000) Flexural cantilever models of extensional subsidence in the Munster Basin (SW Ireland) and Old Red Sandstone fluvial dispersal systems. Geological Society, London, Special Publications 180(1): 239-268

Williams RA (1991) The Berehaven copper mines. British Mining No. 42, The Northern Mine Research Society, Sheffield U.K.

Wilson WH, Powell S (1956) Historic mining map, Allihies Copper Mines (Co. Cork), Mountain Mine. Geological Survey of Ireland, GSI Goldmine.

https://secure.dccae.gov.ie/goldmine/docpage.html?id1=8264207&id2=24780680&id3=24780686. Accessed 8 May 2017

Figure captions

Fig. 1. Simplified map of the Munster Basin and the South Munster Basin in Southwest Ireland. The northern margin of the Munster Basin is defined by the Coomnacronia-Killarney-Mallow Fault Zone (CKMFZ) or alternatively by the Dingle Bay-Galtee Fault Zone (DB-GFZ). The Cork-Kenmare Fault Zone (CKFZ) indicates the rim to the South Munster Sub-Basin (modified from MacCarthy *et al.* (Geological Survey of Ireland) 2002; Williams 2000; Landes *et al.* 2003; MacCarthy 2007; Ennis *et al.* 2015).

Fig. 2. Left: Overview of the historic copper mines around Allihies Village on the western end of Beara Peninsula. Right: Zoom into the mining area at Mountain Mine, showing the bedrock geology, major structures, alteration zones and the traces of mapped underground workings (modified from Reilly 1986; historic mining map, Allihies Copper Mines 1919).

Fig. 3. (**a**) The major lodes and mineralised veins of the Mountain Mine Area with pre-deformation structures. High-resolution drone maps and Bing™ Satellite Maps (2016), including field analysis and modifications from Reilly (1986). (**b**) Outcrop of pre-Variscan, extensional faults (graben structure) at the western end of Mountain Mine E-W Lode. The southern fault is filled with a quartz-chlorite vein ($V_{extensional}$ = 020/70), which is deformed (syn-Variscan) by competent sandstone layers (Sst) and incompetent siltstones (Sltst). Syn-Variscan, compressional veins ($V_{compressional}$ = 033/79) occur at the northern part of the outcrop.

Fig. 4. Equal angle stereoplots of structural features of the Allihies Mining District showing the poles according to the measured planar structures (Key: Kamb contours in standard deviation, interval 2, significance level 3; created with Stereonet (Allmendinger *et al.* 2013, Cardozo and Allmendinger 2013)). (**a**) Mineralised quartz veins. (**b**) Smaller E-W quartz veins. (**c**) Cleavage $S_{1,\ host}$ of the host rock sediments. (**d**) Bedding-cleavage intersection lineations showing steep plunge. (**e**) Bedding of the host rock sediments (Caha Mountain Formation). (**f**) Jointing within the host rock sediments.

Fig. 5. 3D model of the major lodes and the underground workings at Mountain Mine. This model is a combination of a drone photogrammetry model, Bing™ Satellite Maps (2016), metadata for the SRTM digital terrain model (Jarvis *et al.* 2008) and historic mining plans (Wilkinson and Powell 1956).

Fig. 6. Photographs of pre-Variscan structures observed in the field of the Allihies Mining District**:** Outcrop at Marion Lode showing 3 different vein generations (G1-G3) in the siltstone (Sltst). The dip direction of the lode is V = 015/78. The magnification inset (left) shows anticlockwise rotated vein clasts and corrugations (black arrows) on the vein surface, which indicate strike slip movement. The magnification (right) shows the 3rd vein generation (G3) cross-cutting the previous generations with a sub-horizontal orientation.

Fig. 7. Map with syn-Variscan structures affecting the pre-Variscan faults and veins (drone maps and Bing™ Satellite Maps (2016), including field analysis and modifications from Reilly (1986)). (**a**) The major lodes of the Mountain Mine Area with pre- and syn-deformation structures. (**b**) Is showing the sinistral faulted lode of Great Mountain Mine (NW of Mountain Mine Area, see Fig. 2). (**c**) Sinistral faulting of Coom Lode (ESE of Mountain Mine, see Fig. 2).

Fig. 8. Field observations of the syn-Variscan structures at Allihies. (**a**) Cleavage (dip direction $S_{1,\ vein}$ = 113/83) within the Northern Lode of Great Mountain Mine. (**b**) Smaller E-W vein north of Mountain Mine displaying the cleavage within the vein ($S_{1,\ vein}$ = 283/59) and the cleavage of the hosting siltstone $S_{1,\ host}$ = 324/79 which aligns parallel to the vein orientation V = 001/89. (**c**) Cataclastic deformation at the eastern end of Coom Lode. (**d**) Syn-compressional saddle reef quartz veins occurring at the fold axis of second order folds.

Fig. 9. Microphotographs of samples from the Allihies Mining District. (**a**) Mineralised quartz (Qz) veins within fine grained siltstone (Sltst) show syntaxial elongate blocky crystals with cogenetic chalcopyrite (Ccp) (xpl, Mountain Mine Underground). (**b**) Historic quartz (Qz) vein with molybdenite (Mol). The sample was collected by Sir Arthur Russell in 1918 (BM.1964,R231; National History Museum of London). The smaller microscopic image (top right) shows the syngenetic intergrowth of molybdenite (Mol) with chalcopyrite (Ccp) within the quartz (Qz) vein. (**c**) Paragenetic sequence of the pre-Variscan minerals within the quartz veins at the Allihies Mining District.

Fig. 10. Mineralised E-W veins collected North of Mountain Mine (samples 418). The figure shows the E-W strike of the veins (dip direction V = 184/90), their cleavage $S_{1,\ vein}$ = 279/75 and the cleavage of the hosting, fine grained siltstone $S_{1,\ host}$ = 321/80. The false colour microphotographs were captured (xpl) from thin sections (>30 µm) cut perpendicular to the vein cleavage $S_{1,\ vein}$ = 279/75. **Vein A** is a syntaxial quartz vein with elongate blocky crystals. **Vein B1** shows elongate blocky crystals with a cataclastic zone of smaller, subhedral crystals to the northern vein boundary (the colour change at the southern part of B1 is caused by image stitching effects). The magnification shows N-S striking intergranular secondary fluid inclusion trails. In **vein B2**, the elongate blocky crystals are cross-cut by a cataclastic zone to the northern grain boundary and one in the middle of the vein. The magnification shows a micro en echelon vein which indicates sinistral movement. **Vein B3** shows intensive brecciation of the elongate blocky crystals.

Fig. 11. Fluid inclusions from samples of the Allihies District. (**a**) Plot of the salinity wt% $NaCl_{equiv}$ versus the homogenisation temperatures T_h (°C). The points indicate early extensional vein samples and the triangles are measurements from syn-compressional veins. (**b**) Histogram of the eutectic melting $T_{first\ melt}$ (°C) from early extensional veins and from syn-Variscan veins.

Fig. 12. Schematic model of the vein development, mineralisation and structural evolution of the Munster Basin and South Munster Basin (not to scale). (**a**) North-South extension listric subsidence and alluvial sedimentation into the Munster and South Munster Basin. Active Extensional Faults, parallel aligned to the Cork-Kenmare Fault, provide fluid pathways for the precipitation of mineralised quartz veins. (**b**) Syn-Variscan compression causes cleavage, folding and faulting of the basin sediments. Cleavage development within early

extensional quartz veins and sinistral faulting. Formation of syn-compressional saddle reef and en echelon veins.

Supplementary material:

- Video file: 3D model of the major lodes and the underground workings at Mountain Mine (see Fig. 5). This model is a combination of a drone photogrammetry model, Bing™ Satellite Maps (2016), metadata for the SRTM digital terrain model (Jarvis *et al.* 2008) and historic mining plans (Wilkinson and Powell 1956).
- Excel spreadsheet: Fluid inclusions measurements of the Allihies Copper Mining District. Locations are as shown in Fig. 2 and 7.
- Excel spreadsheet: Sample locations of the Allihies Copper Mining District.

Table 1. *Re-Os isotope data for the molybdenite sample (BM.1964,R231) from Allihies Mountain Mine (Fig. 3)*

Sample	*Sample wt (g)*	*Re (ppm)*	±2*σ*	^{187}Re *(ppm)*	±2*σ*	^{187}*Os (ppb)*	±2*σ*	*Model age (Ma)**	±2*σ*†	±2*σ*‡	±2*σ*§
BM.1964,R 231, Mountain Mine	0.010	43.9	0.2	27.6	0.1	169.1	0.8	366.4	0.2	1.5	1.9
Caminches Mine	0.011	3.83	0.04	2.41	0.03	14.78	0.16	367.3	0.2	5.4	5.5

All data blank corrected (Re – 1.9 pg, Os – 0.8 pg with an $^{187}Os/^{188}Os$ of 0.201 ± 0.03)

*Model age calculated using the decay constant ^{187}Re = 1.666×10^{-11} a^{-1} (Smoliar et al., 1996; Selby et al., 2007)

†uncertainty including only mass spectrometry uncertainty

‡uncertainty including all sources of analytical uncertainty

§uncertainty including all sources of analytical uncertainty plus decay constant

figure 1

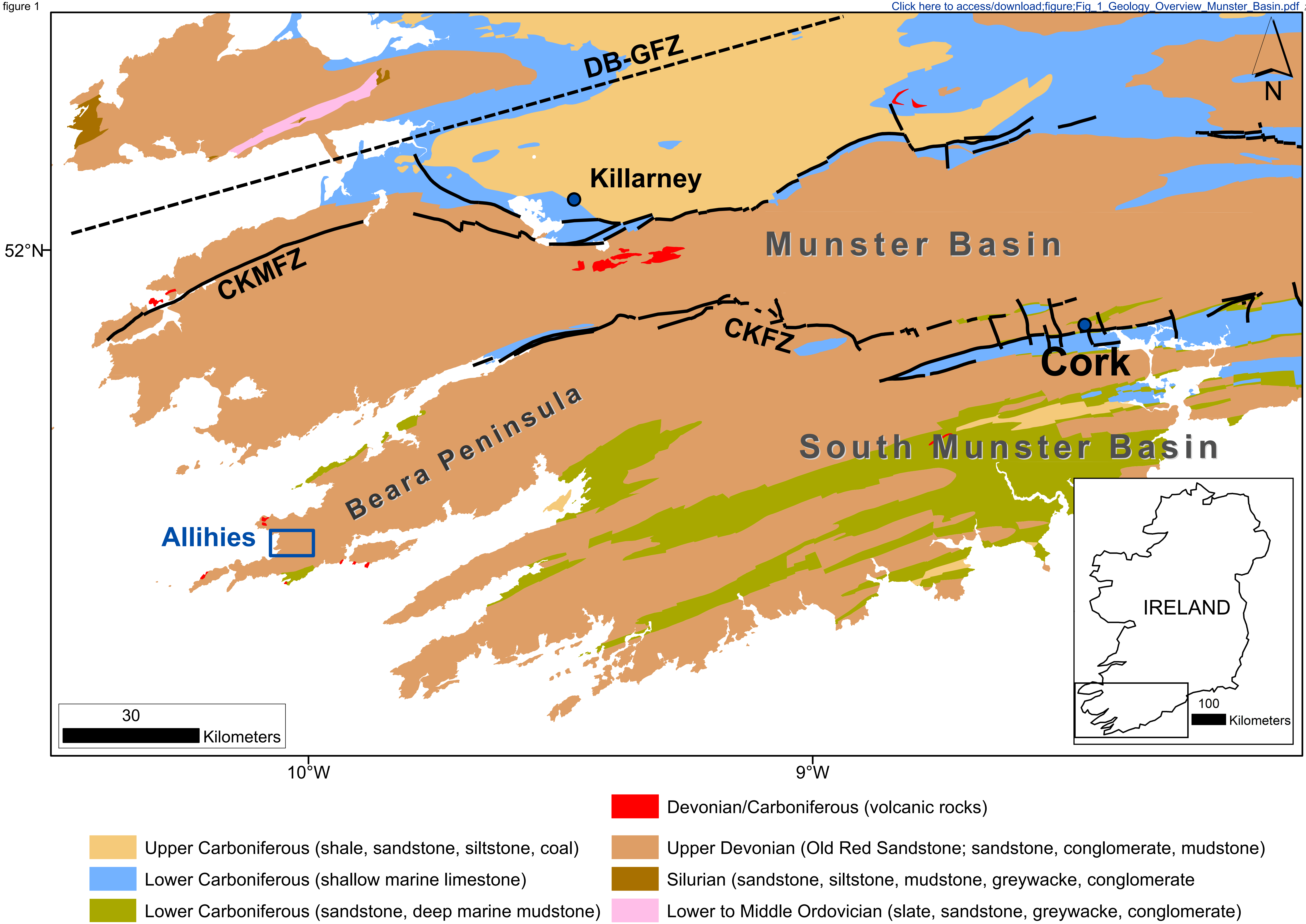
DB-GFZ
Killarney
Munster Basin
CKMFZ
CKFZ
Cork
Beara Peninsula
South Munster Basin
Allihies
N
52°N
10°W
9°W
30
Kilometers
IRELAND
100
Kilometers
Devonian/Carboniferous (volcanic rocks)
Upper Carboniferous (shale, sandstone, siltstone, coal)
Lower Carboniferous (shallow marine limestone)
Lower Carboniferous (sandstone, deep marine mudstone)
Upper Devonian (Old Red Sandstone; sandstone, conglomerate, mudstone)
Silurian (sandstone, siltstone, mudstone, greywacke, conglomerate
Lower to Middle Ordovician (slate, sandstone, greywacke, conglomerate)

figure 2

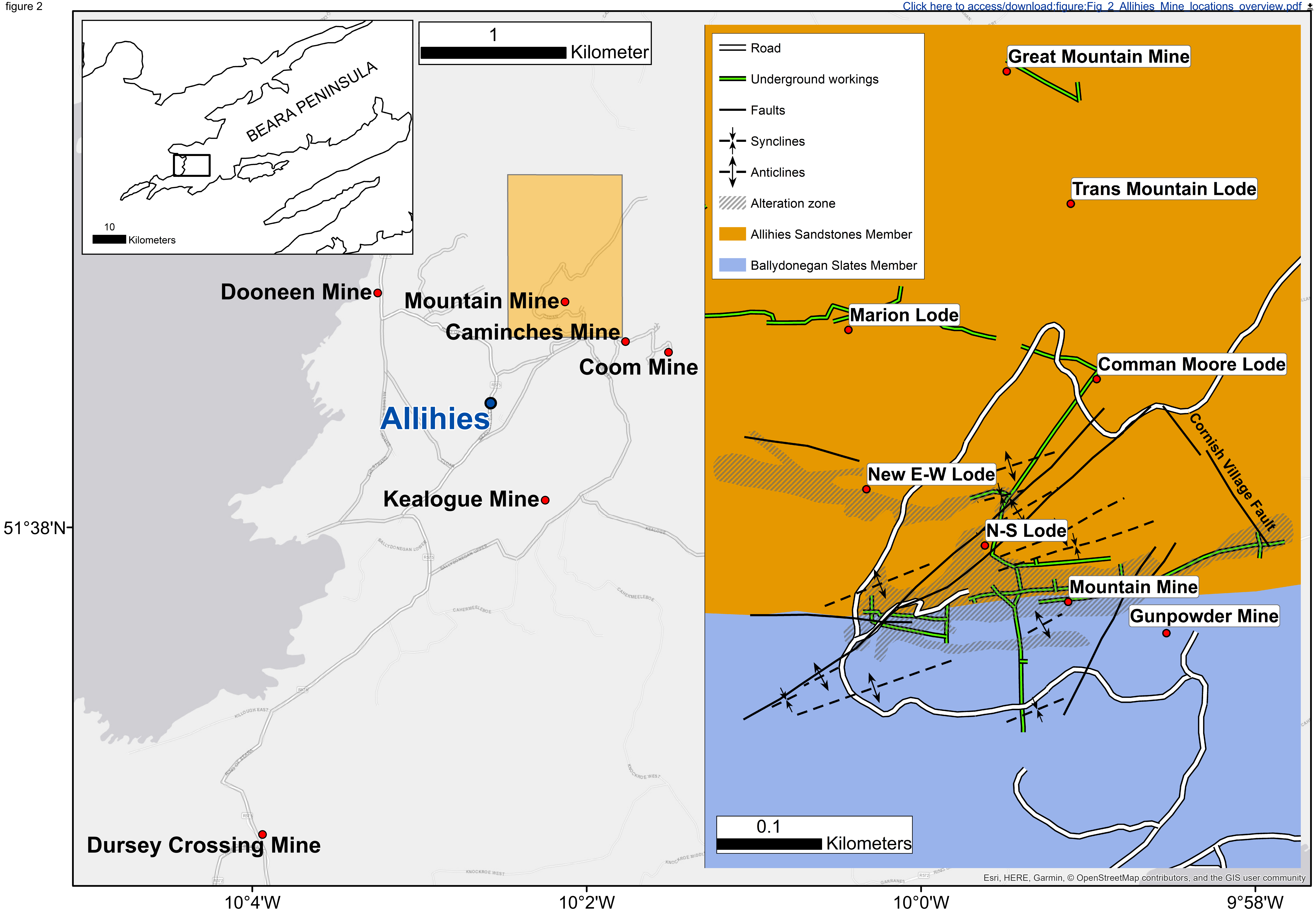
BEARA PENINSULA
10
Kilometers
1
Kilometer
Road
Underground workings
Faults
Synclines
Anticlines
Alteration zone
Allihies Sandstones Member
Ballydonegan Slates Member
Great Mountain Mine
Trans Mountain Lode
Marion Lode
Comman Moore Lode
Cornish Village Fault
New E-W Lode
N-S Lode
Mountain Mine
Gunpowder Mine
0.1
Kilometers
Dooneen Mine
Mountain Mine
Caminches Mine
Coom Mine
Allihies
Kealogue Mine
Dursey Crossing Mine
51°38'N
10°4'W
10°2'W
10°0'W
9°58'W
Esri, HERE, Garmin, © OpenStreetMap contributors, and the GIS user community

figure 3

Click here to access/download;figure;Fig_3_Allihies_Map_Pre_V

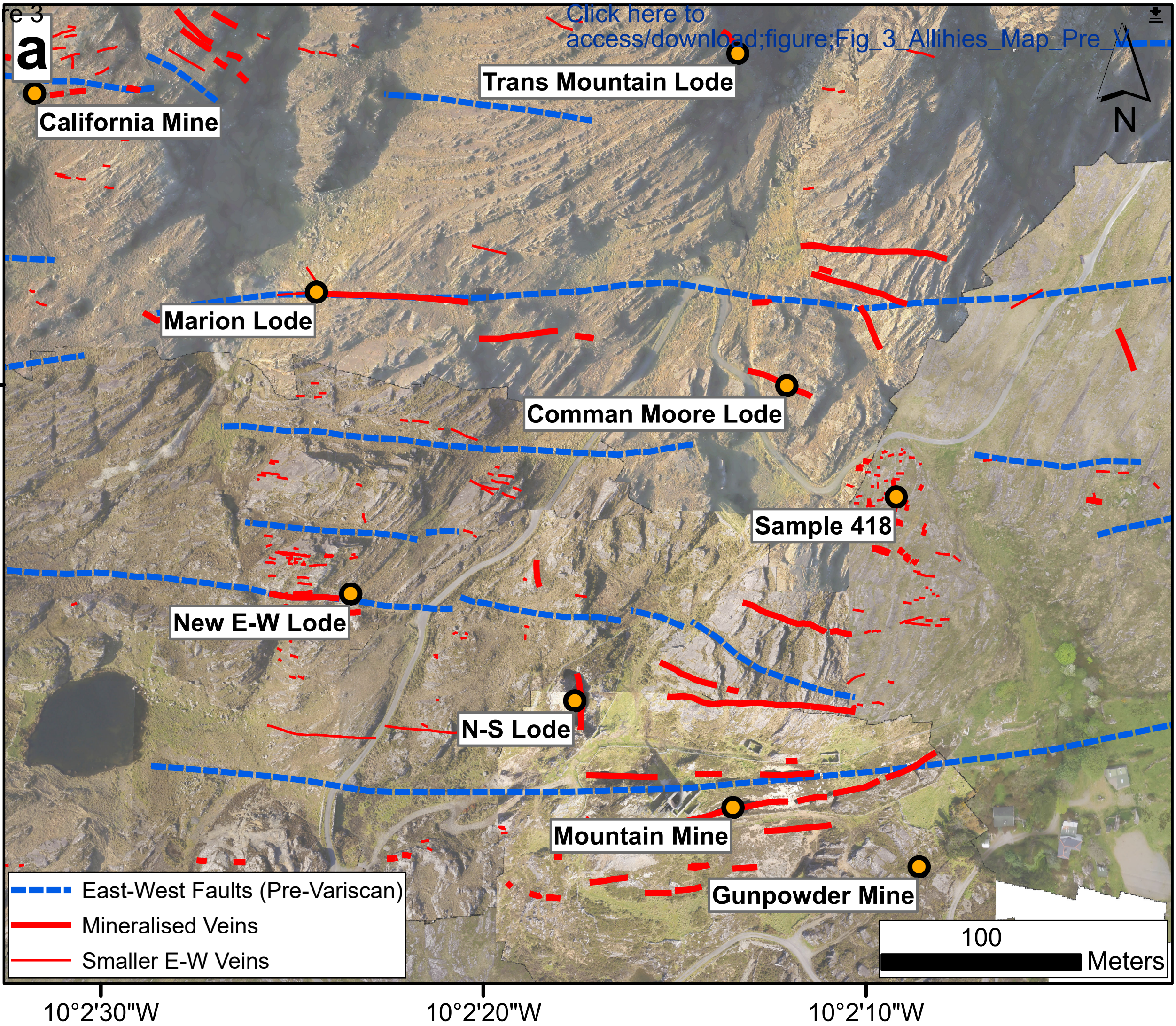

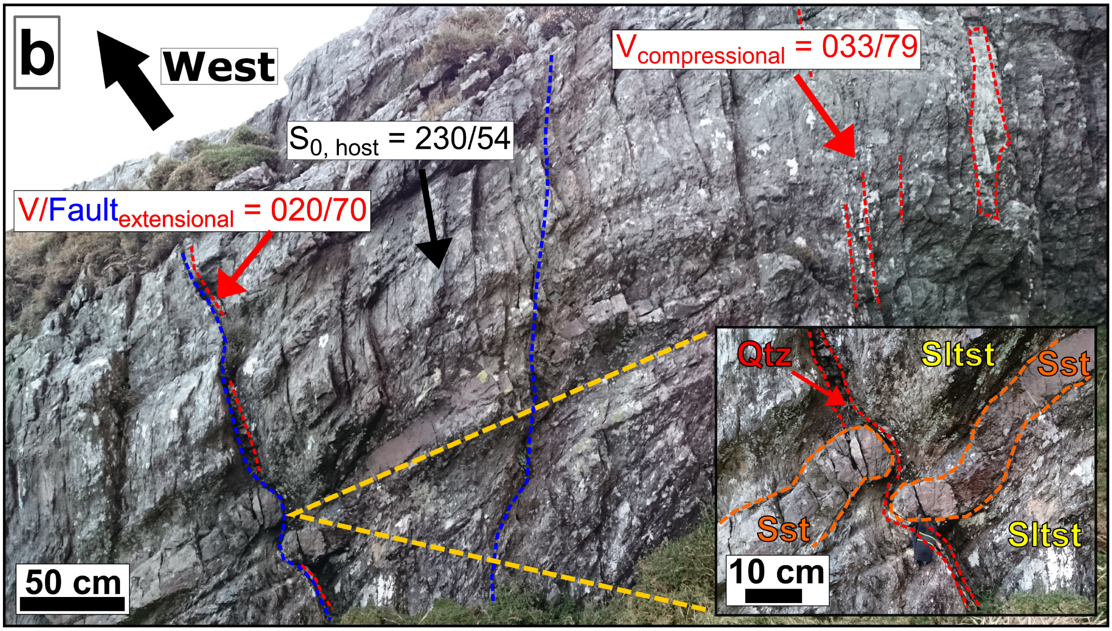

figure 4

Click here to access/download;figure;Fig_4_Stereoplots_Structures.pdf

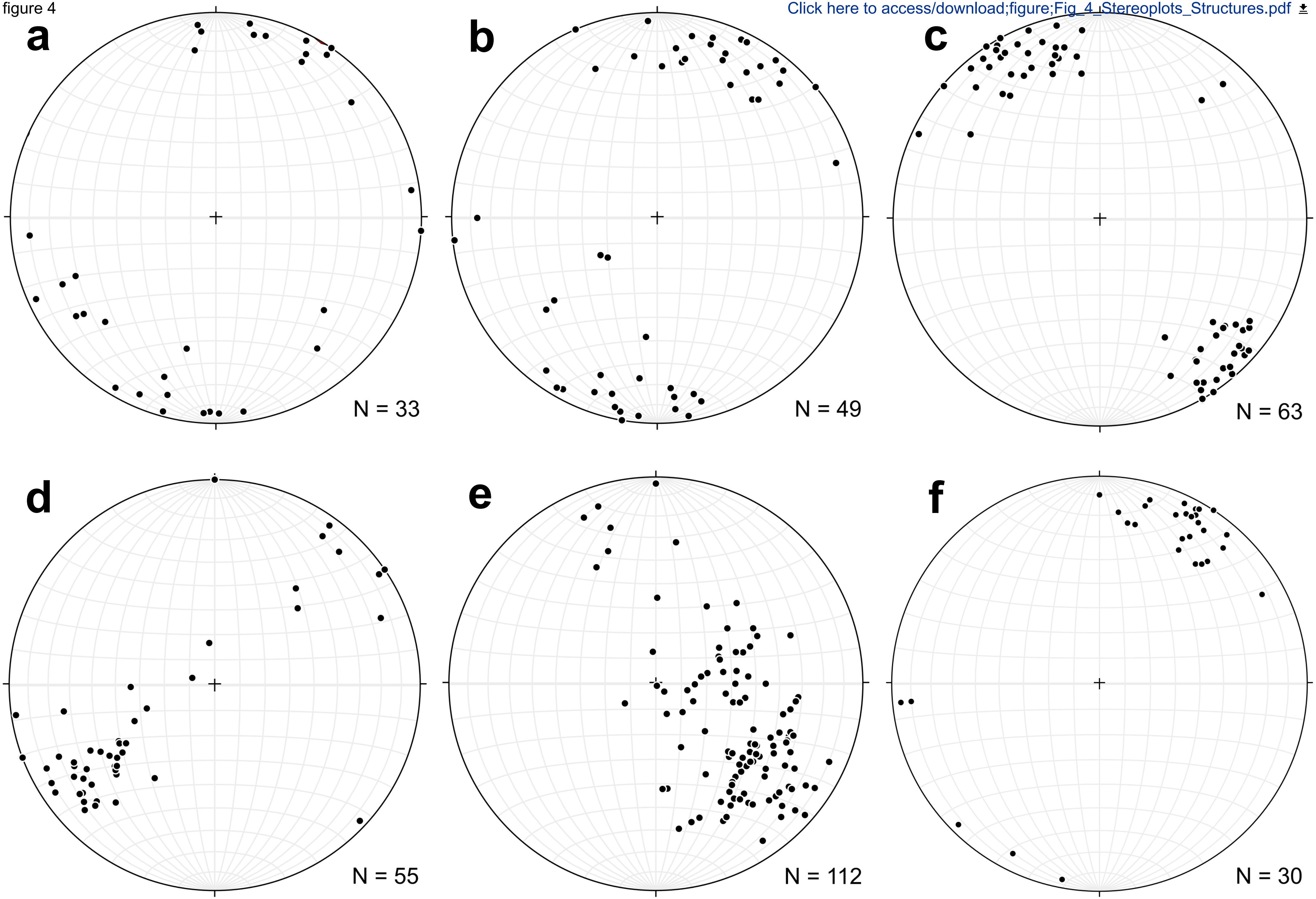

figure 5

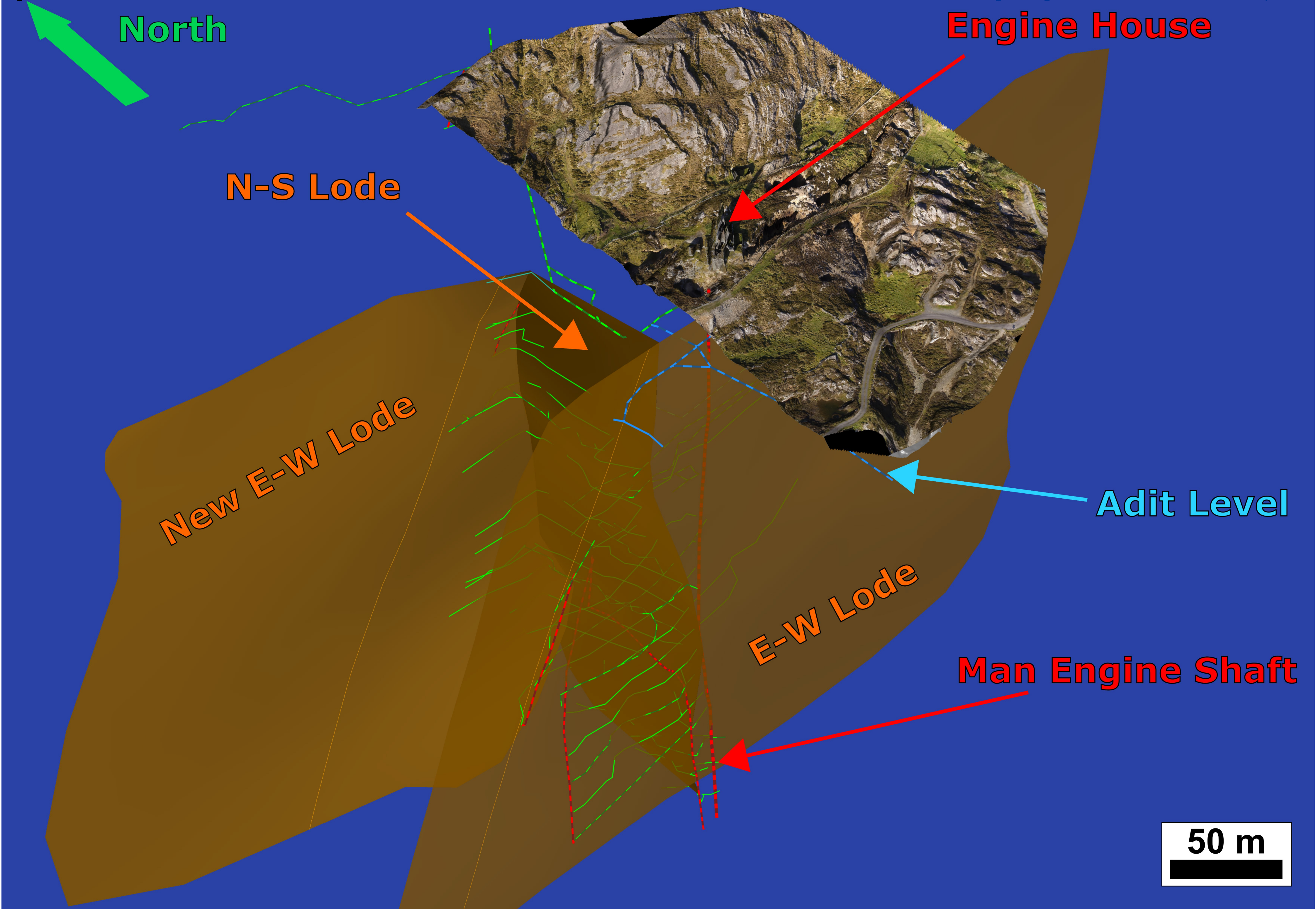
North
Engine House
N-S Lode
New E-W Lode
Adit Level
E-W Lode
Man Engine Shaft
50 m

10 cm
Sltst
V = 015/78
East
G3
G1
G1
G1
G1
G1
G2
G2
G2
G2
Sltst
3 cm
10 cm
G3

figure 7

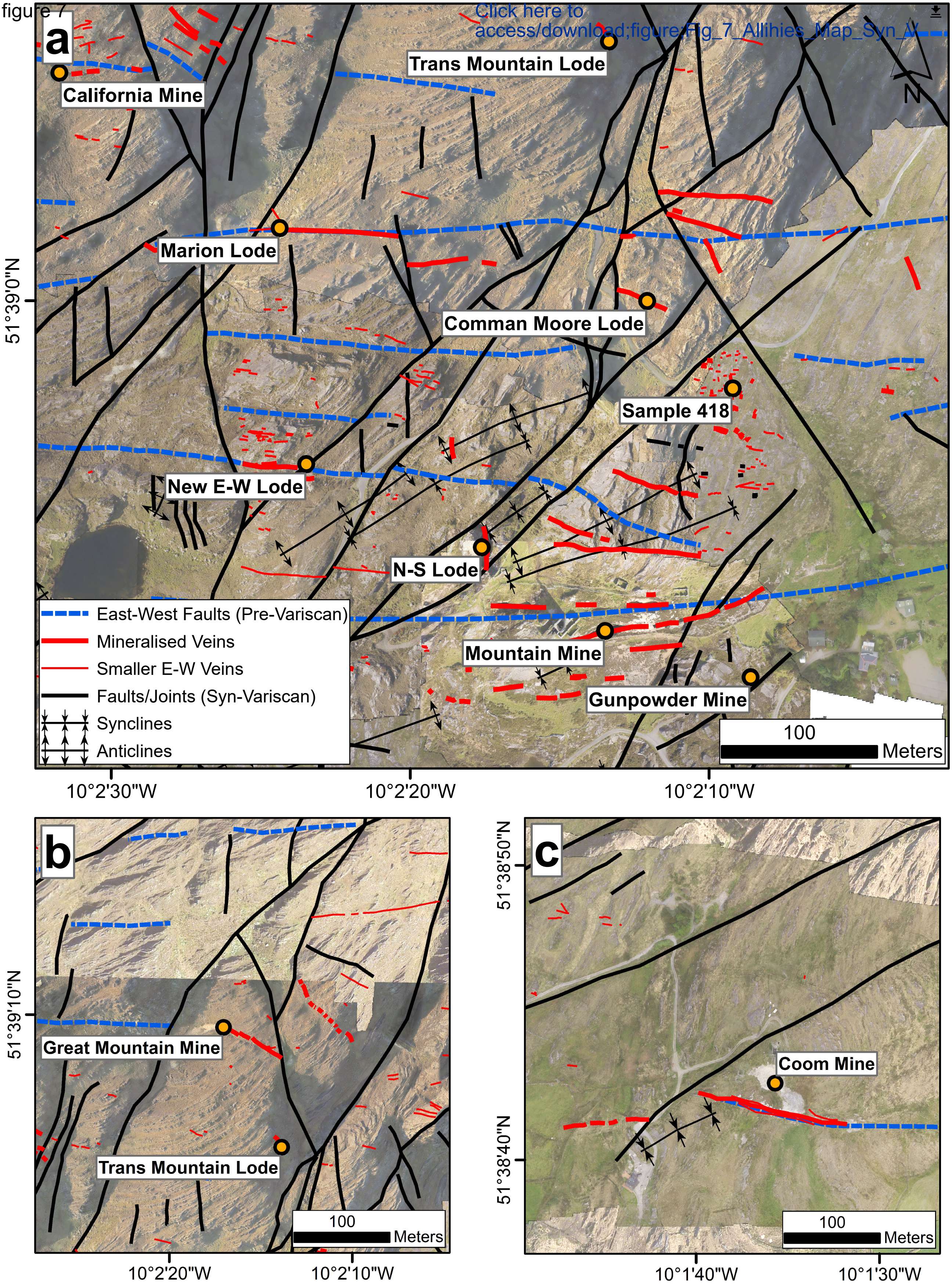
a
California Mine
Trans Mountain Lode
N
Marion Lode
Comman Moore Lode
Sample 418
New E-W Lode
N-S Lode
Mountain Mine
Gunpowder Mine
East-West Faults (Pre-Variscan)
Mineralised Veins
Smaller E-W Veins
Faults/Joints (Syn-Variscan)
Synclines
Anticlines
100
Meters
51°39'0"N
10°2'30"W
10°2'20"W
10°2'10"W
b
Great Mountain Mine
Trans Mountain Lode
100
Meters
51°39'10"N
10°2'20"W
10°2'10"W
c
Coom Mine
100
Meters
51°38'50"N
51°38'40"N
10°1'40"W
10°1'30"W

figure 8

Click here to access/download;figure;Fig_8_Field_Observations_Lower_Resolution.pdf

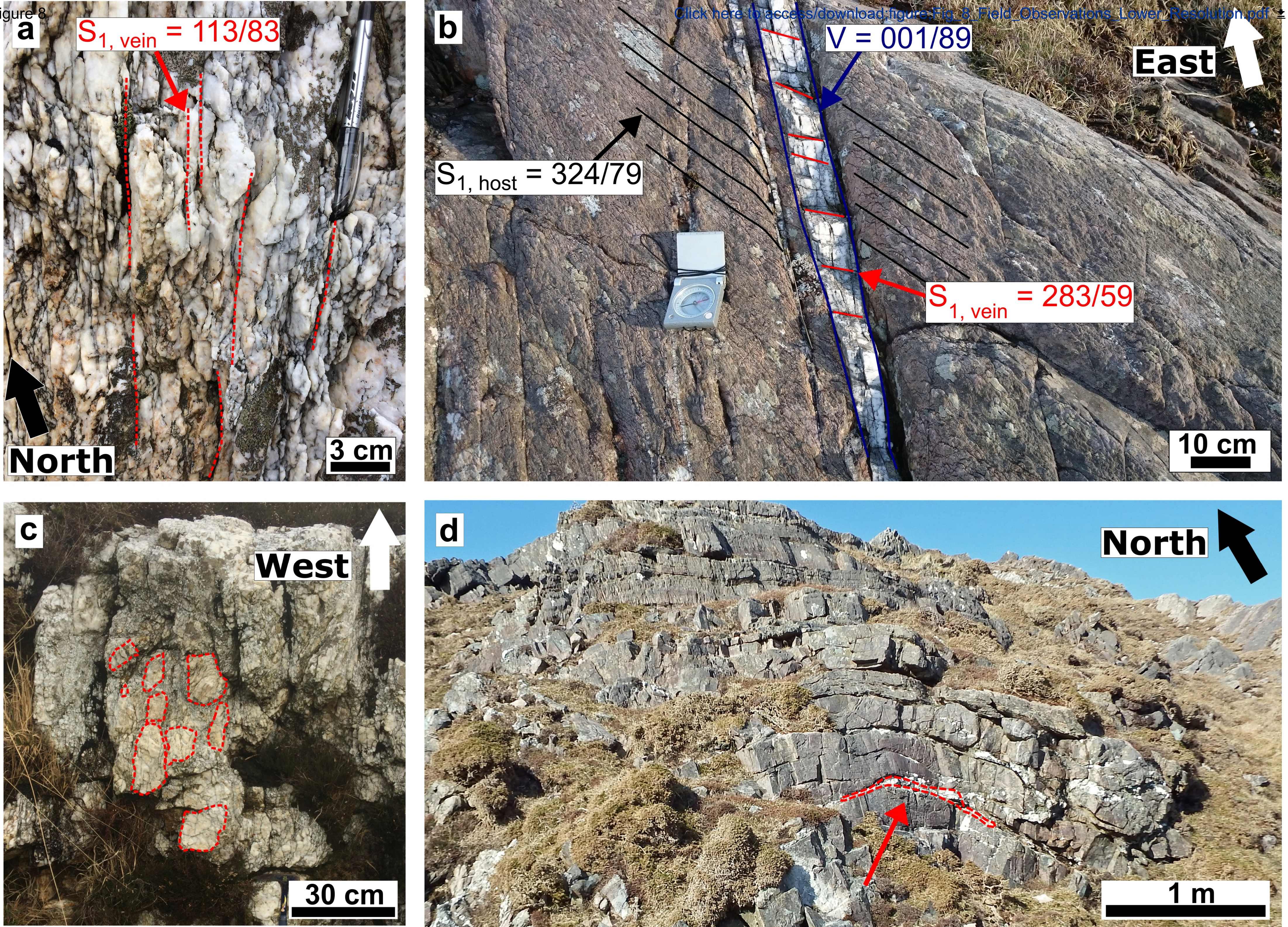

figure 9

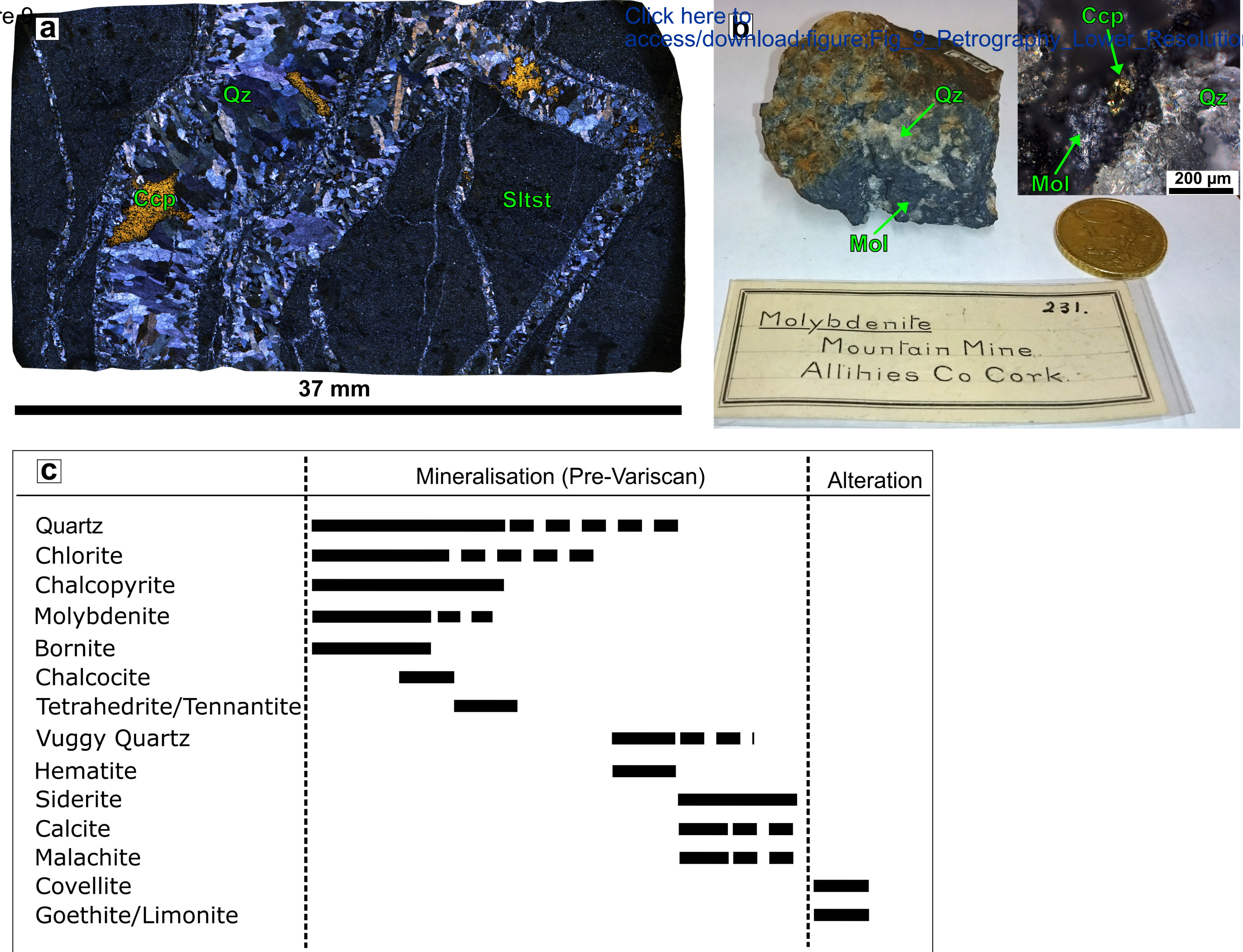
a
Qz
Ccp
Sltst
37 mm
b
Qz
Mol
Ccp
Qz
Mol
200 µm
231.
Molybdenite
Mountain Mine
Allihies Co Cork.
c
Mineralisation (Pre-Variscan)
Alteration
Quartz
Chlorite
Chalcopyrite
Molybdenite
Bornite
Chalcocite
Tetrahedrite/Tennantite
Vuggy Quartz
Hematite
Siderite
Calcite
Malachite
Covellite
Goethite/Limonite

figure 10

Click here to access/download;figure;Fig_10_Sample_418_Microstructures.

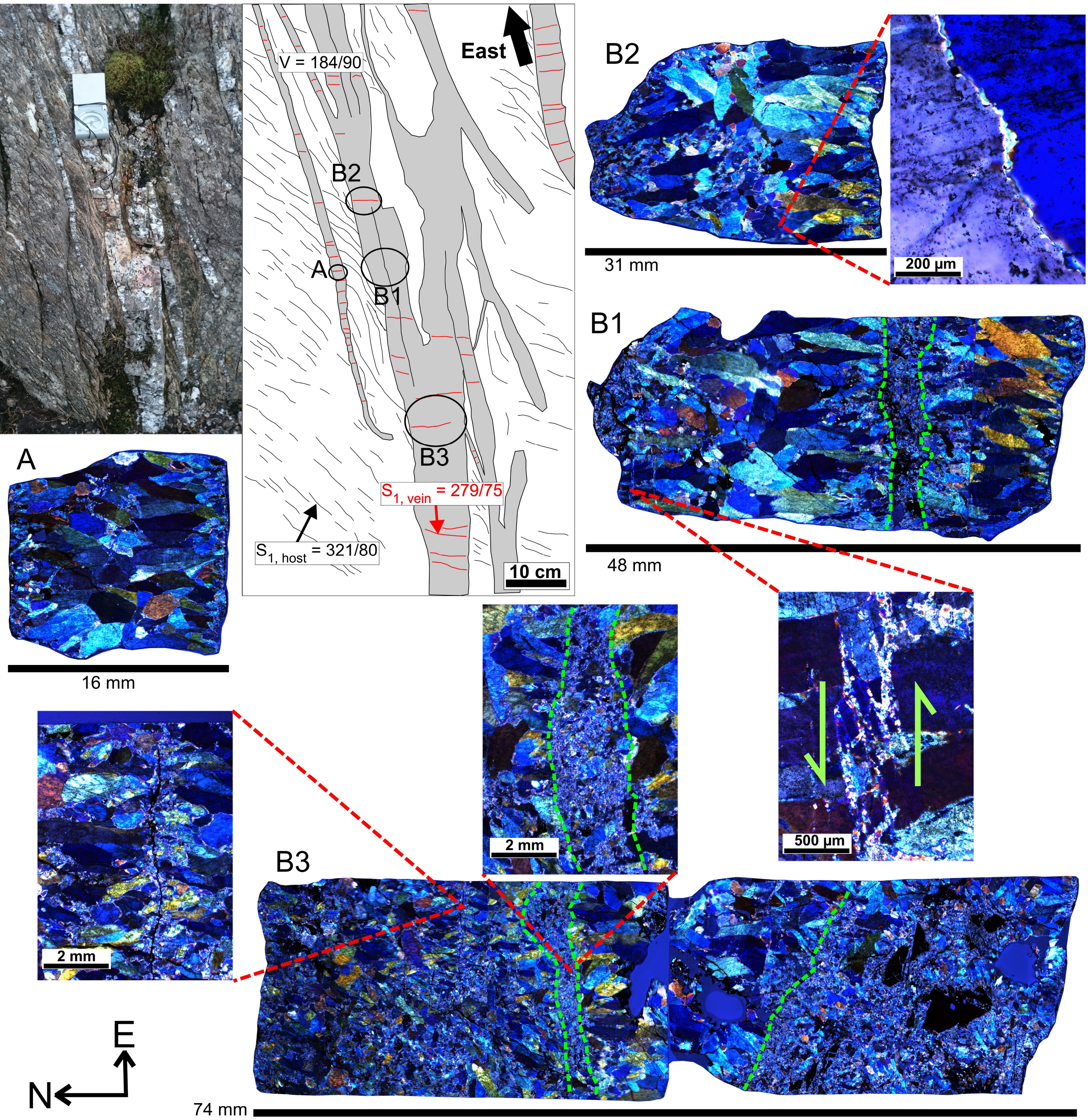

figure 11

Click here to access/download;figure;Fig_11_Fluid_Inclusions.pdf

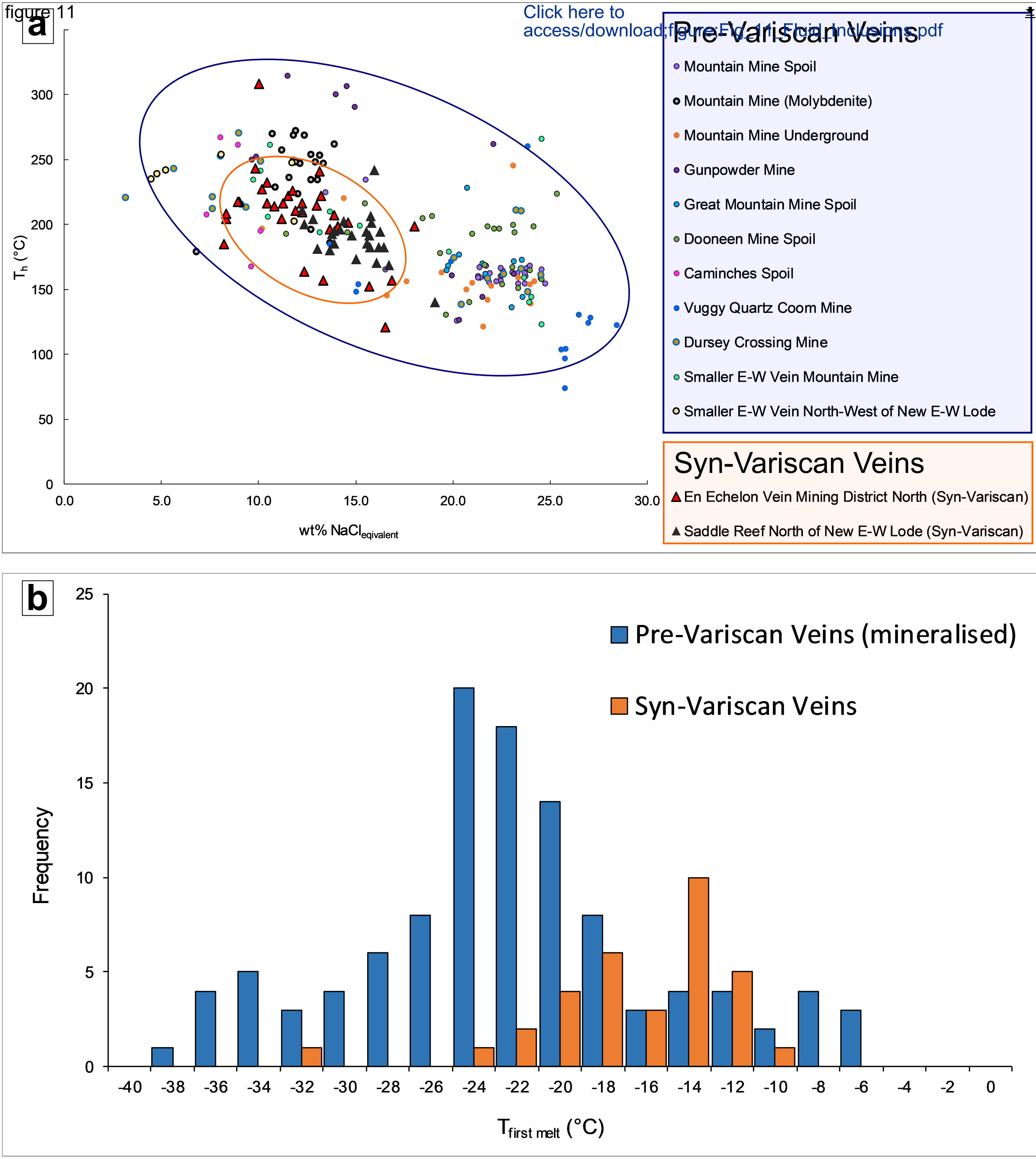

figure 12

Click here to access/download;figure;Fig_12_Block_Model.pdf